

4.1 INTRODUCTION

Separation membranes have become essential components in hi-tech areas such as biotechnology, nano-technology and membrane based energy devices in addition to different membrane based separation and purification processes. These processes are highly economically viable due to low energy requirements and facile scale-up of membrane modular design. Advances in membrane technology, especially in novel materials, can make this technology even more competitive with traditional processes that are high-energy intensive, environmentally undesirable and costly.

Ion exchange membranes are one of the most advanced separation membranes. Ion exchange membrane technologies are non-hazardous in nature and are being widely used not only for separation and purification but their application is also extended towards energy conversion devices, storage batteries, sensors etc. There is now a great demand for ion exchange membranes with better selectivity, less electrical resistance, high chemical, mechanical and thermal stability as well as good durability.

For these wide applications, the most desired properties required for successful ion exchange membranes are:

- ❖ High perm selectivity — an ion exchange membrane should be highly permeable to counter ions, but should be impermeable to co-ions.
- ❖ Low electrical resistance — an ion exchange membrane should have low electrical resistance so that there is less potential drop during electro membrane processes.
- ❖ Good mechanical stability — the membrane should be mechanically strong and should have a low degree of swelling or shrinking in transition from dilute to concentrated ionic solutions.
- ❖ High chemical stability — the membrane should be stable over a pH-range from 0 to 14 and in the presence of oxidizing agents.

Properties of some commercially available membranes are listed in (**Table 4.1**) [1–7]. This table, however, is far from being complete and subject to rapid change.

Table 4.1 Properties of commercial ion exchange membranes [1-7]

| Membrane | Structure properties | IEC [meq/g] | Thickness [mm] | Water content [%] | Area resistance [$\text{h}\Omega\text{cm}^2$] | Perm-selectivity [%] |
|---|---------------------------|-------------|----------------|-------------------|---|----------------------|
| <i>Tokuyama Soda Co. Ltd. Japan</i> | | | | | | |
| Neosepta CMX | Cation, PS/DVB | 1.5-1.8 | 0.14-0.20 | 25-30 | 1.8-3.8 | 97 |
| Neosepta AMX | Anion, PS/DVB | 1.4-1.7 | 0.12-0.18 | 25-30 | 2.0-3.5 | 95 |
| Neosepta CMS | Cation PS/DVB | 2.0 | 0.15 | 38 | 1.5-2.5 | - |
| Neosepta ACM | Anion PS/DVB | 1.5 | 0.12 | 15 | 4.0-5.0 | - |
| <i>Asahi Glass Co. Ltd. Japan</i> | | | | | | |
| CMV | Cation PS/DVB | 2.4 | 0.15 | 25 | 2.9 | 95 |
| AMV | Anion PS/butadiene | 1.9 | 0.14 | 19 | 2.0-4.5 | 92 |
| HJC | Cation heterogeneous | 1.8 | 0.83 | 51 | - | - |
| <i>Ionic Inc., USA</i> | | | | | | |
| 61CZL386 | Cation heterogeneous | 2.6 | 0.63 | 40 | 9 | - |
| 103PZL183 | Anion heterogeneous | 1.2 | 0.60 | 38 | 4.9 | - |
| <i>Dupont Co., USA</i> | | | | | | |
| Nafion 117 | Cation fluorinated | 0.90 | 0.20 | 16 | 1.5 | 97 |
| Nafion 901 | Cation fluorinated | 1.1 | 0.4 | 5 | 3.8 | 96 |
| <i>RAI Research Corp., USA</i> | | | | | | |
| R-5010-H | Cation LDPE/HDPE | 0.9 | 0.24 | 20 | 8.0-12.0 | 95 |
| R-5030-L | Anion LDPF | 1.0 | 0.24 | 30 | 4.0-7.0 | 83 |
| R-1010 | Cation fluorinated | 1.2 | 0.10 | 20 | 0.2-0.4 | 86 |
| R-1030 | Anion fluorinated | 1.0 | 0.1 | 10 | 0.7-1.5 | 81 |
| <i>Institute of Plastic Materials, Moscow</i> | | | | | | |
| MA-40 | Anion | 0.6 | 0.15 | 17 | 5.0 | 95 |
| <i>CSMCRI, Bhavnagar, India</i> | | | | | | |
| IPC | Cation LDPE/HDPE | 1.4 | 0.14-0.16 | 25 | 1.5-2 | 97 |
| IPA | Anion LDPE/HDPE | 0.8-0.9 | 0.16-0.18 | 15 | 2.0-4.0 | 92 |
| HGC | Cation, PVC Heterogeneous | 0.67-0.77 | 0.22-0.25 | 14 | 4.0-6.0 | 87 |
| HGA | Anion, PVC Heterogeneous | 0.4-0.5 | 0.22-0.25 | 12 | 5.0-7.0 | 82 |

4.2 MEMBRANE SYNTHESIS

The parameters, determining the membrane properties, often have an opposing effect. For example, a high degree of cross-linking improves the mechanical strength but increases the electrical resistance, while more ionic charges in the membrane matrix lead to a low electrical resistance, but in general, cause a high degree of swelling combined with poor mechanical stability. Thus there is a compromise between these properties to develop good ion exchange membranes.

Regarding chemical structure, ion exchange membranes are very similar to ion exchange resins because both bear functional groups. The difference between membranes and resins arises largely from the mechanical requirement of the membrane process. Unfortunately, ion exchange resins are mechanically weak, cation resins tend to be brittle, and anion resins soft. They are dimensionally unstable due to the variation in the amount of water imbibed into the gel under different circumstances. Changes in electrolyte concentration, and temperature may cause major changes in the water uptake and hence in the volume of the resin. These changes can be tolerated in small spherical beads. However, in large sheets that have been cut to fit an apparatus, they are not acceptable. Thus, it is generally not possible to use sheets of material that have been prepared in the same way as a bead resin. The most common solution to this problem is the preparation of a membrane with a backing of a stable reinforcing material that gives the necessary strength and dimensional stability. Most of the commercial ion exchange membranes can be divided into two major categories, according to their structure and preparation procedure: homogeneous and heterogeneous.

Nano structured inorgano-organic composite materials [8-18] are currently objecting tremendous research because of their versatile properties of mechanically stable inorganic backbone and the specific chemical reactivity of the organic-functional group. These interesting properties of new materials are dependent on their structural and chemical composition as well as on the dynamical properties inside the blend.

Thus, in the investigation processes, inorganic material should be accommodated in the organic matrix in such a way that it should permit the utilization of maximum elementary functions in a small volume, and hence optimize complementary possibilities and properties of the inorganic and organic components. Thus ionic membranes with ordered two dimensional ion conducting channels vertically aligned to the membrane surface with excellent mechanical, chemical and dimensional stability as well as flexibility is an urgent need.

Sol-gel processing is one of the promising routes to synthesis of membrane materials using a “Chimie Douce”, low temperature approach. Using sol-gel route, it is possible to introduce a large variety of organic moieties into an inorganic matrix.

Ion exchange membranes, both homogeneous and heterogeneous, being unique in their nature, overcome each other in one way or another. Homogeneous membranes having good electrochemical properties, lack in their mechanical strength, whereas heterogeneous membranes having very good mechanical strength are comparatively poor in their electrochemical performance [19]. However, by choosing a suitable binder to make non-reinforced membranes or by choosing a suitable reinforcing fabric, it is possible to have good ion exchange membranes by an optimum combination of electrochemical properties and mechanical strength.

Heterogeneous ion exchange membranes can also be made by mechanical incorporation of powdered ion exchange resin into sheets of rubber, PVC, acrylonitrile copolymers or some other extrudable or mouldable matrix. Such membranes can be prepared [20] either by (a) calendaring ion exchange particles into an inert plastic film or (b) dry moulding of inert film forming polymers and ion exchange particles and then milling the mould stock or (c) resin particles can be dispersed in a solution containing a film forming binder and then the solvent is evaporated to give ion exchange membrane [8]. Such heterogeneous membranes may also be reinforced with a chemically resistant fabric [21].

Sensitive and mature technologies for the removal of heavy metal ions from aqueous solutions is an important scientific endeavour during recent years [22]. Several separation methods such as ion exchange resin [23,24], ion selective electrode [25,26], liquid membrane separation [27,28], polymer inclusion membranes [29-31], neutral ionophore based crown ether [32-34], ion exchange membrane based technology [35-41], etc, are available in the literature.

Many of these technologies have suffered because of poor mechanical strength, low chemical stability, high cost as well as low selectivity or efficiency. Ion exchange membranes are stepping over and above all of them and making a great market boom due to their comparatively high durability, mechanical stability, chemical sustainability, selectivity, ionic conductivity [42] along with low cost and maintenance expense. Stable and specific metal ion selective membranes with controlled IEC, surface charge density, hydrophilicity/hydrophobicity and porosity, are extremely desirable for the removal of metal ion contamination. Inorgano-organic nanocomposite membranes with fascinating properties like mechanical and thermal

stability, specific chemical reactivity and flexibility, have great potential to solve many problems in separation and purification engineering [11, 12, 14 43-45].

Lately lot of attention is focussed towards preparing hybrid inorgano-organic based ion exchange membranes, because of compatibility between the properties of both organic and inorganic constituents, which make specific ion selective separation membrane.

In Chapter-III of the thesis the use of ZrD and ZrT as amphoteric exchangers has been accomplished.

4.3 AIM AND SCOPE OF THE PRESENT WORK

The increasing contamination of surface and ground water by heavy metal ions is a worrying environmental problem. Inorganic pollutants are of considerable concern because they are highly toxic, non-biodegradable, get accumulated in living tissues, and cause various diseases and disorders [46, 47]. Industrial activities such as, metal plating, mining activities, smelting, battery manufacture, tanneries, petroleum refining, paint manufacture, pesticides, pigment manufacture, printing and photographic industries cause a waste water mixture of heavy metal ions [48,49]. Conventional techniques for metal ion abatement, are chemical precipitation, ion-exchange [23, 24], electro-floatation [50], polymer inclusion membranes [27], membrane separation [28, 33, 35, 36, 40] and solvent extraction [34, 42]. In spite of simplicity and cost effective nature of adsorption process, regeneration of adsorbents require huge water, acid and base, which further creates industrial wastes. However, high process cost and low efficiency are still problems. Furthermore, it is difficult to fractionate the mixture of heavy metal ions for their reutilization. To overcome these problems, developments of specific selective membranes/ materials are required, which shows comparatively low load, high durability, and chemical sustainability, needed for reutilization of waste and hazardous material [51]. Thus, it is desirable to develop specific selective membrane-based process for selective recovery/differentiation of heavy metal ions.

Copper (Cu^{2+}) is of particular interest because of its toxicity and industrial applications. Recovery of Cu^{2+} in presence of other impurities (Ni^{2+} , Zn^{2+} , and Mn^{2+}) have been rarely studied [52]. According to current practice, removal/fractionation of these heavy metal ions requires the use of harmful chemicals, which is serious and accompanied by economical/environmental disadvantages [53]. Materials containing

chelating ligands are used in many applications, because of their specific selectivity for transition metals [54]. Chelating adsorbents containing poly(ethyleneimine) and 2-(aminomethyl)pyridine were used for selective separation of Cu^{2+} [52]. Some studies also focused on chelating/adsorptive membranes, with surfaces anchored with $-\text{SO}_3\text{H}$, $-\text{COOH}$ or $-\text{NH}_2$ groups (able to form surface complex with heavy metal ions) [55, 56]. Chitosan based adsorptive membranes were reported for removal of heavy metal ions due to availability of amine ($-\text{NH}_2$) functional groups [57, 58]. However, selective separation/recovery of Cu^{2+} in presence of other heavy metal ions are less studied. Ligand (triethylenetetramine) modified thin film membranes were also employed as selective adsorbents because of ideal host lattice and complexing agent to form complex with Cu^{2+} [59, 60].

In Chapter-III of the thesis it was observed that zirconium tri-ethylene tetra-amine (ZrT) amphoteric exchanger exhibits specific selectivity for Cu^{2+} due to presence of amine groups. Incorporation of ZrT gel into polymer matrix by sol-gel ensures the formation of homogeneous and interconnected polymer network. Herein, we report Cu^{2+} selective chelating ZrTETA-X membranes, suitable for the recovery of Cu^{2+} in presence of other bi-valent metal ions. These membranes have been employed in an electro-driven process based on the principles of electrodialysis for separating Cu^{2+} in presence of other bi-valent metal ions.

4.4 OBJECTIVES OF THE PRESENT WORK

In the present study hybrid chelating membranes, based on cross-linked zirconium tri-ethylene tetra-amine (ZrT) gel and poly vinyl alcohol (PVA) has been reported. The ZrT chelating membranes have been designated as ZrTETA-45, ZrTETA-50 and ZrTETA-55, based on different weight percentage of ZrT gel used to prepare the membranes. The chelating membranes have been synthesized by an acid catalyzed sol-gel process followed by chemical crosslinking via formal reaction. The membranes have been subjected to, (a) Physicochemical methods of characterization which include, water uptake, swelling, ion exchange capacity (IEC), fixed-ion concentration, oxidative stability and hydrolytic stability. (b) Electrochemical methods of characterization which include, transport number, membrane conductivity, electro-osmotic permeability and metal ion transport studies. (c) Instrumental methods of characterization which include spectral analysis (ATR-FTIR), thermal analysis

(TGA/DSC), DMA, XRD, SEM and EDX. Metal ion transport studies have been performed for different bivalent ions namely Mn^{2+} , Ni^{2+} , Cu^{2+} and Zn^{2+} . The experiments have also been carried out using mixed metal electrolyte (equi-molar) for achieving separations.

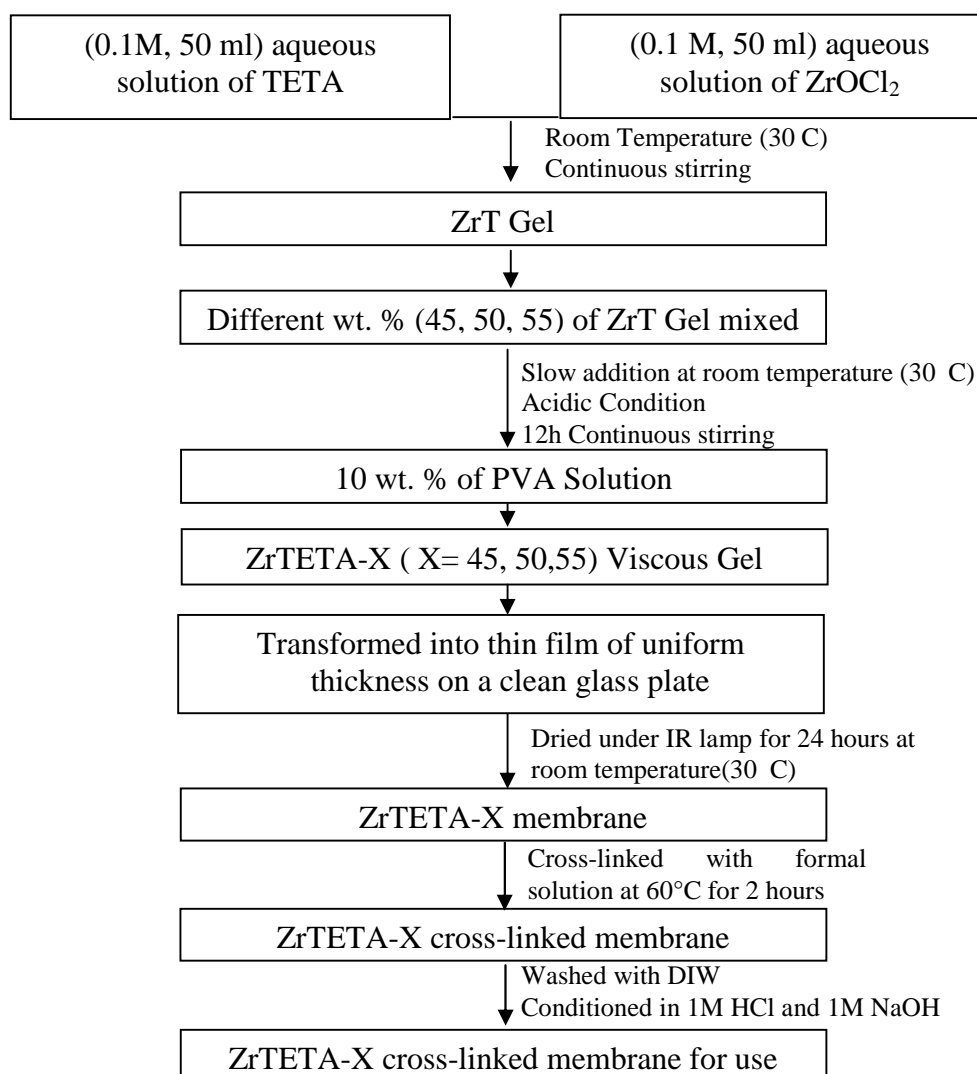
Amongst the chelating membranes prepared of varying gel composition, crosslinked ZrTETA-55 hybrid chelating membrane exhibits strong interaction towards all metal ions, specially Cu^{2+} . Thus, thermodynamic, kinetic and adsorption studies were performed using ZrTETA-55 chelating membrane which involves effect of time, temperature, pH, adsorbent dose, and adsorbate concentration, towards adsorption of Cu^{2+} . Pseudo-first and pseudo second order kinetic models, thermodynamic parameters {(Standard free energy (UG°), enthalpy (UH°) and entropy (US°)} have been evaluated and adsorption isotherms (Langmuir and Freundlich) studied.

4.5 EXPERIMENTAL

Materials and Methods: Tri-ethylene tetra-amine (TETA) ($C_8H_{18}N_4$ Mw =146.24 and Density=0.970 g/ml) and Zirconium oxychloride ($ZrOCl_2 \cdot 8H_2O$) were procured from Loba Chemicals, India. Poly(vinyl alcohol) (PVA, Mw: 125000; degree of polymerization: 1700, degree of hydrolysis: 88%), methanol, formaldehyde, hydrogen peroxide, Na_2SO_4 , NaCl etc. of AR grade were received from S.D. fine chemicals, India and used without any further purification. Chloride and nitrate salts of transition metal ions (Mn^{2+} , Ni^{2+} , Cu^{2+} , Zn^{2+}) of AR grade were obtained from E Merck, India. Indicators and reagents used are of AR grade. Deionized Water (DIW) was used in all experiments.

Membrane Preparation: ZrT gel was prepared by drop wise mixing of aqueous solution of TETA (0.10 M, 50 ml) and $ZrOCl_2$ (0.10 M, 50 ml) at 30 °C under continuous stirring, when white gelatinous precipitate was obtained. ZrTETA-PVA hybrid membrane was prepared by acid catalyzed sol–gel route followed by chemical crosslinking via formal reaction. A 10 wt. % of PVA solution was prepared in DIW at room temperature under stirring. ZrT gel (inorganic precursor) of fixed weight percentage was slowly mixed with PVA solution. The solution was stirred at room temperature under acidic conditions for 12 h to obtain a viscous gel. The resulting gel was transformed into thin film of uniform thickness on a clean glass plate and dried

under IR lamps at ambient temperature for 24 h followed by vacuum drying at 60 °C for the next 12 h. This film was further cross linked with formal solution (HCHO+H₂SO₄ in1:1.6 v/v ratios in water) at 60 °C for 2 h. The resulting membrane was washed thoroughly using DIW and conditioned in 1.0 M HCl and NaOH solutions, successively. Finally, the conditioned membranes were stored for further studies. Membranes with different weight percentage of ZrT were prepared and designated as ZrTETA-X, (where, X = 45, 50 and 55 wt. % of ZrT gel) (**Scheme-1**, Synthesis of ZrTETA-X cross linked membrane).



Scheme 1 *Synthesis of ZrTETA-X cross linked membrane*

4.6 CHARACTERIZATION OF ION EXCHANGE MEMBRANES

The properties of ion exchange membranes are determined by two parameters, namely the basic polymer matrix and the nature and concentration of fixed ionic moiety. The basic polymer matrix determines to a large extent the mechanical, chemical and thermal stability of the membrane, while the concentration of the fixed ionic charges determine the permselectivity and electrical resistance of the membrane but they also have significant effect on the mechanical properties of the membrane [53, 61-63].

4.6.1 Mechanical Properties of Ion Exchange Membranes

The mechanical characterization of ion exchange membranes include- the determination of thickness, swelling, dimensional stability, tensile strength and hydraulic permeability. All tests are carried out with pretreated and well equilibrated membranes. Hydraulic permeability measurements provide information on the transport of components through a membrane under hydrostatic pressure driven forces. The presence of pinholes in ion exchange membranes not only leads to a drastically increased hydraulic permeability but also invalidates any application. Pinholes can be determined by placing a wet membrane sheet on a sheet of white absorbent paper. A 0.2 % solution of methylene blue for an anion exchange membrane or a 0.2 % solution of erythrocein-B for a cation exchange membrane has to be spread over the entire surface. If no spot of the dye is observed on the paper, the membrane is free of pinholes and can be tested for its hydraulic permeability. The test is carried out at room temperature using DIW and a hydrostatic pressure driving force. The permeability can be calculated from the volumetric flow rate. The swelling capacity of a membrane determines not only its dimensional stability but also affects its selectivity, electrical resistance and hydraulic permeability. It depends on the nature of the polymeric material, the ion exchange capacity and the cross-linking density [61-63].

4.6.2 Physicochemical Methods of Characterization

Water uptake: To assess the hydrophilicity of membranes, water uptake is evaluated from difference in weight of the membranes before and after hydration. Membrane is immersed in DIW for 24 h to make it saturated and its wet weight is recorded after removing surface water thoroughly. Weight of dry membrane is recorded after drying

the membrane completely under vacuum at 60 °C for 12 h. The water uptake of the membrane matrix (ϕ_w) is determined by following equation:

$$\phi_w(\%) = \frac{W_{wet} - W_{dry}}{W_{dry}} \times 100 \quad (\text{Eq. 4.1})$$

where, W_{wet} and W_{dry} are the weight of the membrane under wet and dry conditions.

The water uptake is determined as weight percentage from the weight of the dry and wet sample. Water content in terms of water concentration in the membrane phase is determined by means of the following equation [64, 65]:

$$C_w^m = (W_h - W_d)\rho_m / W_h M_w \quad (\text{Eq. 4.2})$$

where C_w^m designates the concentration of water in the membrane, W_h the wet membrane weight, W_d the dry membrane weight, ρ_m the density of wet membrane and M_w the molar mass of water (18 g mol⁻¹).

The membrane porosity (τ (volume of free water within membrane per unit volume of wet membrane)) can be obtained by following equation [60]:

$$\tau = \Delta V / (1 + \Delta V) \quad (\text{Eq. 4.3})$$

where ΔV designates the volume increase of the membrane upon absorption of the water per unit of dry membrane volume, which may be estimated by using following equation:

$$V = (W_h - W_d)\rho_d / \rho_w W_d \quad (\text{Eq. 4.4})$$

where ρ_d is the density of dry membrane and ρ_w is the density of water, which enters into the membrane. Usually the swelling of a membrane is expressed in terms of water content or uptake

Swelling: The dimensional changes in thickness and plane directions are also measured for the wet and dry membranes in order to evaluate the swelling properties by using the following equation:

$$\text{Swelling} (\%) = \frac{V_{wet} - V_{dry}}{V_{dry}} \times 100 \quad (\text{Eq. 4.5})$$

where, V_{wet} and V_{dry} are the volume of the membrane under wet and dry conditions.

Ion exchange capacity (IEC): The ion exchange capacities of charged membranes are determined by titrating the fixed ions, e.g. –SO₃H group with 0.1 N NaOH or HCl, respectively. For these tests, cation and anion exchange membranes are equilibrated for about 6 h in 1 N HCl or NaOH, respectively, and then rinsed free from chloride or sodium ions with DIW. The ion exchange capacity of the sample is then determined

by back titration with 0.1 N NaOH or HCl, respectively. Weak base anion exchange membranes are characterized by equilibration in 1 N sodium chloride and titration with standardized 0.1 N silver nitrate solution. The samples are then dried, and the IEC ($\text{meq}\cdot\text{g}^{-1}$) of the membrane is calculated by [8],

$$IEC = ab/w \quad (\text{Eq. 4.6})$$

where ‘a’ and ‘b’ are the burette reading and concentration respectively of acid, base or silver nitrate and ‘w’ is the dry weight of the membrane (g). Further more, ion exchange capacity can be used for the determination of fixed-ion concentration (X^m) of the membrane in units of (moles of sites) / (unit volume of wet membrane),

$$X^m = \tau(IEC)\rho_d/\Delta V \quad (\text{Eq. 4.7})$$

where τ = membrane porosity, ρ_d = density of dry membrane and ΔV = volume increase of the membrane upon absorption of the water per unit of dry membrane volume.

In the present study ion exchange membrane was equilibrated in 1.0 M HCl/1.0 M NaOH for 24 h to ensure that all charged sites of the membranes are in H^+ / OH^- form and washed with DIW to remove traces of acid/base. The washed membranes were then equilibrated in 0.5 M NaCl solutions for 24hr. Ion-exchange capacity was determined from the increase in basicity/acidity and amount of OH^- / H^+ liberated, estimated by acid-base titration. The IEC ($\text{meq}\cdot\text{g}^{-1}$) for membrane was calculated using (Eq. 4.6) [45].

Chemical Stability of Membranes: The economics of electro-membrane processes is determined to a large extent by the chemical stability and the life of the ion exchange membranes under applied conditions. Deterioration in polymer matrix or functionality of the ion exchange membranes after exposure for certain time periods to various test solutions containing acids, bases, or oxidizing agents is estimated by visual comparison with new, unexposed samples and by determining changes in their mechanical, dimensional and electrical properties. To explore the stability of these membranes in harsh, oxidative, hot aqueous and acidic environment, long-term aging experiments were carried out in respective mediums. The membranes were tested for oxidative and hydrolytic stability. **Oxidative stability** consists in testing the membrane degradation by oxiactive radicals, by immersing in Fentons reagent (3% H_2O_2 and 3ppm FeSO_4) at 80 °C for 1h [66], while **hydrolytic stability** consists in testing the membrane degradation in hot aqueous medium. Small pieces of membranes were

immersed in boiling water for 24 h at 120 °C in a pressurized closed vial. The oxidative and hydrolytic stability was evaluated by loss in weight, ion-exchange capacity and physical appearance of the test samples [67]. Membrane stability was also accessed in HCl of different concentrations for a fixed time period, and its swelling parameter was recorded. The weight loss fraction (W_0) and fraction change in IEC (IEC_0) by oxidative degradation were obtained by following equations:

$$W_0 = \frac{W_i - W_f}{W_f} \quad (\text{Eq. 4.8})$$

and

$$IEC_0 = \frac{IEC_i - IEC_f}{IEC_f} \quad (\text{Eq. 4.9})$$

where subscript i and f denotes initial and final, respectively.

4.6.3 Electrochemical Methods of Characterization

Electrical Resistance by Electrochemical Impedance Studies: Impedance spectroscopy has been used extensively to determine the electrical resistances of ion exchange membranes by applying alternating current across the membrane under operating conditions [64, 68-70]. Impedance measurement at a single frequency, yields information about the electrochemical properties of the membrane such as variation of frequency and amplitude allows differentiation between single and multilayer systems from the signal response [71]. Signal analysis requires modeling the structure as an interconnected system of capacitances and resistances. Membrane structure has been studied using a four-terminal electrode arrangement across the membranes and porosity of the membrane can be modeled as a skin layer and support layer using the dielectric values of the polymer and the electrolyte solution used [72].

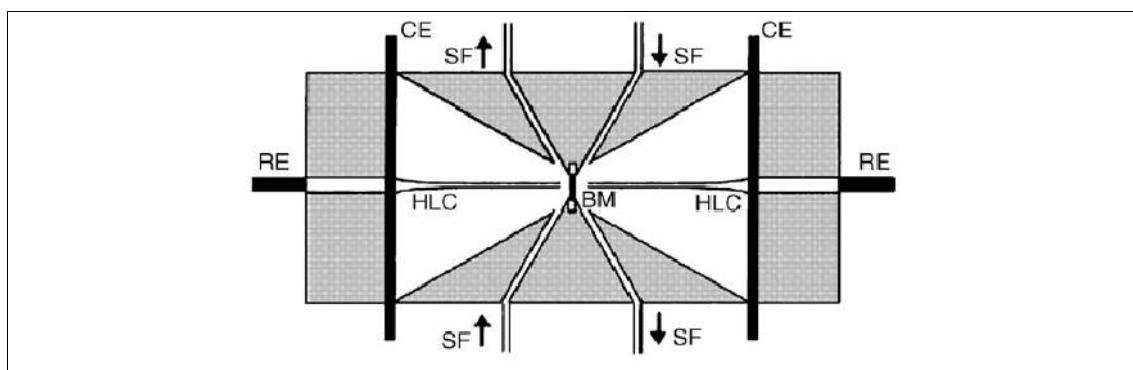


Figure 4.1 *Experimental set up for impedance measurements. Two Ag/AgCl electrodes are used as CEs, and potential across the membrane (BM) is measured with two REs using Haber– Luggin capillaries salt bridges (HLC). The solution flux (SF) is directed to the membrane to avoid concentration changes at interfacial zone*

By varying the frequency and amplitude of the current and measuring the amplitude and phase difference of the electrical potential that develops across it, the dispersions of the conductance and capacitance is used to distinguish between single and multilayer systems, porosity of the system, as well as the changes in the electrochemical processes. Experimental use for the impedance measurements is depicted in **Figure 4.1**, which is a two compartment cell separated by a membrane and consists of two current electrodes (CE) and two reference electrodes (RE).

A membrane in contact and in a state of equilibration with an electrolyte may be described by an equivalent circuit, analogous to that of a Randell cell [73, 74]. For the ideal circuit, frequency dependence of impedance, Z is given by the relationship,

$$Z = R_s + \frac{R_p - j(WR_p^2C)}{1 + (WR_pC)^2} \quad (\text{Eq. 4.10})$$

where, radial frequency $W = 2\pi f$, f is applied frequency, C is the capacitance, R_s is solution resistance, and R_p is interfacial resistance. Z can be written as follows in terms of real (Z_R) and imaginary (Z_I) terms.

$$Z = Z_R + jZ_I \quad (\text{Eq. 4.11})$$

According to (Eq. 4.10), at low frequency limit, the imaginary term vanishes and real term approaches ($R_s + R_p$). At the high frequency limit also imaginary term vanishes and real term approaches R_s . Thus values of R_s and R_p can be estimated using limiting values of impedance at low and high frequency limit.

Impedance measurements have been used with advantages to predict the fouling of ion exchange membranes during electro-membrane processes. The change in the value of the capacitance and resistance measured by impedance spectroscopy during fouling processes or during temperature changes can indicate where the fouling is taking place or where electrochemical or structural changes may be occurring. Fouling of electro dialysis membranes by anionic organic substances (lignosulfonate) has been followed in real time by focusing solely on the capacitance change in the electrical double layer [75]. While the overall capacitance increases, the frequency where it occurs also changes during the fouling process. While impedance spectroscopy has been used to characterize the structural and electrochemical performance of many ion exchange membranes, biological membranes, porous membranes, and proton-exchange membranes, it is unfortunately too difficult a case for polymer membranes, due to the high impedance of the material [76, 77]. However,

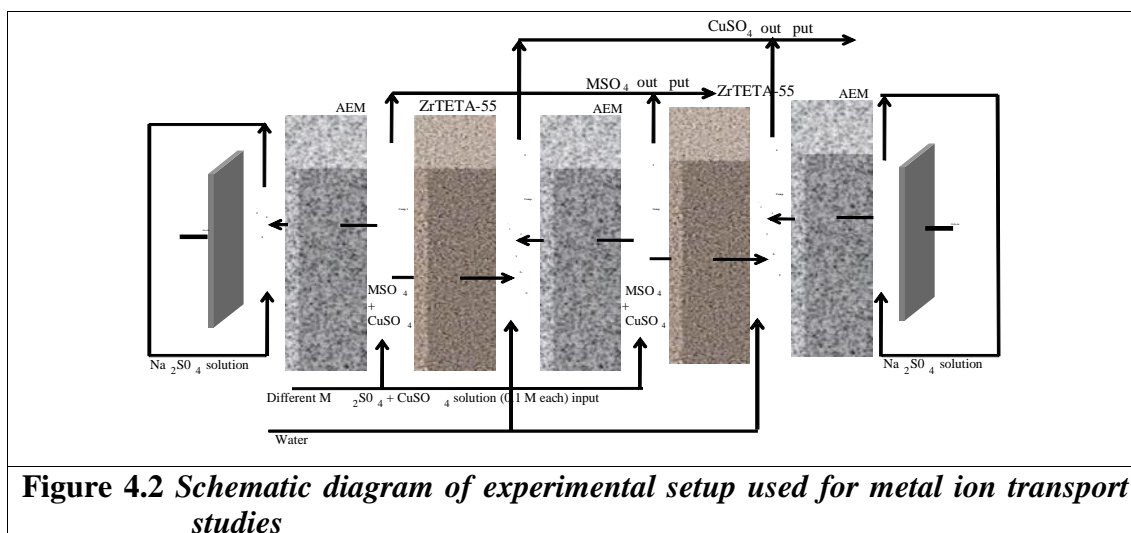
metal-coated membranes have been studied to obtain structural information. Researchers have been able to demonstrate that the structures predicted by impedance measurements are consistent with other techniques such as field emission electron microscopy and atomic force microscopy [78, 79].

Transport number: Counter ion transport number in the membrane phase is obtained by Hittorf method [80, 81]. This dynamic method allows determining the transport numbers under migration. Two asymmetric compartments separated by a circular piece of membrane (7.0 cm²) and electrodes constitute the experimental cell used for the determination of transport number. The cathodic and anodic compartment capacities were 200 ml and 20 ml. Distance between both electrodes and the effective membrane area was 0.11 cm² and 25.0 cm², respectively. Peristaltic pumps were used to feed different metal salt solutions (0.1M) and DIW in a recirculation mode into the cathodic and anodic compartments respectively with constant flow rate. To have a control on the current intensity and voltage, digital multimeter was placed in series to apply the current across the electrodes. The applied current density was 8 mA/cm². Experiments were carried out for 1 h and samples were taken out from the anodic and cathodic compartments and H⁺ ion concentration determined. The counter ion transport number (H⁺) was determined by following equation:

$$t_-^m = \frac{nF}{It} (C^-V^- - C^0V^0) \quad (\text{Eq. 4.12})$$

where n is the charge on hydrogen ion (H⁺), F is the Faraday constant, I is the applied current, t is the time, C^0 and C^- are the initial and final concentrations of H⁺ in the cathodic compartment while, V^0 and V^- are the initial and final volume of cathodic compartment.

Metal Ion Transport Studies: Schematic diagram of the experimental setup used for metal ion transport studies is depicted in **Figure 4.2**. ED cell used for metal ion transport studies contained of two ZrTETA-X membranes and three AEMs divided into six compartments viz., catholyte, anolyte, compartment 1 and 3 (copper metal ion depleted stream), compartment 2 and 4 (copper metal ion enriched stream). All streams were connected through separate tanks to recirculate all streams with the help of peristaltic pumps.



A DC power supply (model L 1285, Aplab, Mumbai, India) was used to apply constant current, while the potential was measured using digital multimeter (model 435, Systronics, India) connected in a series mode. The distances between both electrodes and the effective membrane area were $0.50 \times 10^{-2} \text{ m}^2$ and $8.0 \times 10^{-3} \text{ m}^2$, respectively. Electrodes were made of expanded TiO_2 sheets coated with a triple precious metal oxide (titanium–ruthenium–platinum) (6- μm thickness), with 1.5mm thickness, and obtained from Titanium Tantalum Products (TITAN, Chennai, India). All four storage tanks and pumps were used to feed the different compartments, separately with $6.0 \times 10^{-3} \text{ m}^3/\text{h}$ constant flow rate in batch mode operation. The whole setup was placed at room temperature ($30 \text{ }^\circ\text{C}$) without any additional temperature control. On influence of applied voltage, fed Cu^{2+} migrated from compartments 1 and 3 to 2 and 4 through ZrTETA-55 chelating membrane. With progress of experiment, Cu^{2+} was depleted in compartments 1 and 3, while their concentration was built up in compartment 2 and 4. Similarly, salts of other bi-valent metal ions remained in feed compartment. Experiments were carried out for 2 h and samples were collected from the initial feed and output for estimation of Cu^{2+} and M^{2+} concentration by EDTA complexometric titration in case of single metal transport and by AA-680 Shimadzu atomic absorption/flame emission spectrophotometer in case of mixed metal transport.

Permselectivity: The permselectivity of an ion exchange membrane relates the transport of electric charge by specific counter ions to the total transport of electric charge through the membrane. Ion selectivity of ion exchange membrane is quantitatively expressed in terms of membrane “permselectivity”, which measures the

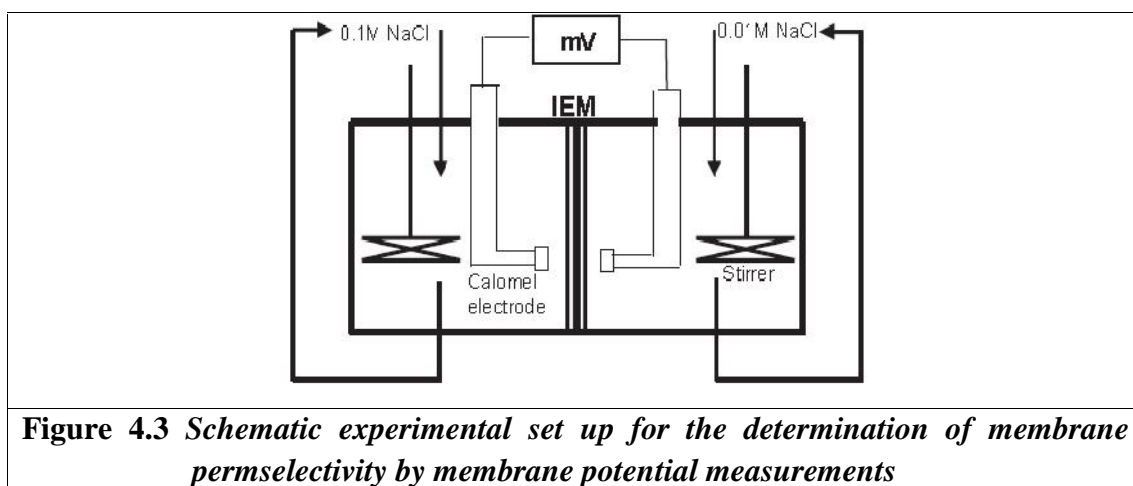
ease with which counter-ion migration occurs through an ion exchange membrane, and is defined as [82-84],

$$P_s = \frac{t_i^m}{1 - t_i} \quad (\text{Eq. 4.13})$$

where, P_s is the permselectivity of the membrane, t_i^m is the counter-ion transport number through the membrane, and t_i is the counter-ion transport number in the solution phase.

An ideal permselective cation exchange membrane would transmit positively charged ions only. The permselectivity approaches zero when the transport number within the membrane is identical to that in the electrolyte solution. Due to the Donnan exclusion, the permselectivity of the membrane depends on the concentration of the electrolytes in the solution and on the ion exchange capacity of the membrane. When a membrane separates dilute and concentrated solutions, there is a concentration gradient across the membrane. In this case the permselectivity is calculated by measuring counter ion transport number across the ion exchange membrane.

Transport number is determined by two methods (i) Hitorf's method (ii) chronopotentiometric method. A faster method for the determination of apparent permselectivities is based on membrane potential measurement. The experimental set-up for the membrane potential measurement is shown in **Figure 4.3**.



The advantage of the determination of potential between two solutions of different concentrations is that the tests are not obscured by concentration polarization effect at the membrane surface. The potential difference between two solutions of the same electrolyte but different concentration can be derived from the general flux equation and for the boundary conditions $P = 0$ and $I = 0$ (i.e. $\sum n_i F_j n_i = 0$) and by introducing several approximations, such as negligible osmotic flow between the two

solutions, constant ion mobilities and small concentration gradients across the membrane phase, etc. The potential difference between solutions can be expressed for a monovalent electrolyte by (Eq. 4.14) [85-87].

$$E^m = (1 - 2t_i^m) \frac{RT}{F} \ln \frac{a_1}{a_2} \quad (\text{Eq. 4.14})$$

where E^m is the potential difference between two solutions containing a monovalent electrolyte (superscript m refers to the membrane), t_i^m is the transport number, a_1 and a_2 are activities of electrolyte solutions, R is gas constant, T is temperature and F is Faraday constant.

Membrane Conductivity: Membrane conductivity measurements for ZrTETA-X membranes equilibrated in different electrolytic environment (0.01 M) were carried out using a potentiostat/galvanostat frequency response analyzer. The membranes were sandwiched between two in house made stainless steel circular electrodes (4.0 cm²). Direct current (dc) and sinusoidal alternating currents (ac) were supplied to the respective electrodes for recording the frequency at a scanning rate of 1 μA/s within a frequency range of 10⁶ to 1Hz. The membrane resistances were obtained from Nyquist plots (a plot of Z_{img} versus Z_r in an impedance plan).

Electro-osmotic permeability: Electro-osmotic permeability measurements were carried out by equilibrating 0.01 M NaCl solutions, in a two-compartment cell (25 cm³), made of acrylic glass and separated by anion exchange membrane (AEM) (24.0 cm²) [88]. Both the compartments were kept under constant agitation by means of a mechanical stirrer. A known potential was applied across the membrane using Ag/AgCl electrodes, and subsequently volume flux was measured by observing the movement of liquid in a horizontally fixed capillary tube of known radius. The current flowing through the system was also recorded with the help of a digital multimeter. Several experiments were performed to obtain reproducible values. Electro-osmotic permeability (P_e) is expressed by,

$$P_e = \frac{\omega XF}{\chi_0 \kappa^m} \quad (\text{Eq. 4.15})$$

where, X is the concentration of fixed ionic charge in the membrane matrix, F = Faraday constant, χ_0 is the specific friction co-efficient between the moving liquid and walls of the membrane pores, κ^m is the specific membrane conductivity and $\omega = -1$ and $+1$, for negatively or positively charged membranes.

Metal ion adsorption studies: Adsorption studies were carried out using batch process. Dry ZrTETA-X membranes (0.1 g) were placed in 20 mL of different electrolytic solutions of (10 mM) concentration in conical flasks for 24 h at room temperature in a shaker incubator at 100 rpm. Ionic concentrations in the supernatant solution were determined by EDTA titration to estimate the adsorbed amount of ions. Measuring error for the estimation of metal ion concentration was 0.1 mg/L.

4.6.4 Instrumental methods of characterization

FT-IR spectrum of ZrT gel particle were recorded by KBr technique on a Shimadzu (model 8400S) in the range of 4000-400 cm^{-1} , while ATR technique was used for dried membranes using spectrum GX series 49387 spectrometer in the range of 4000-600 cm^{-1} . ^1H NMR spectra was also used to elucidate the ZrT structure and obtained using NMR spectrometer (Bruker 500 MHz) in a D_2O solvent. For scanning electron microscopy (SEM), gold sputter coatings were carried out on desired membrane samples at pressure ranging between 1 and 0.1 Pa. Sample was loaded in the machine, operated at 102 to 103 Pa vacuum with EHT 15.00 kv with 300 V collector bias. SEMs were recorded by Leo microscope. The thermal degradation and stabilities of ZrT particles and ZrT composite membranes were investigated using a thermo gravimetric analyzer (TGA, Mettler Toledo TGA/SDTA851with Starc software) under N_2 atmosphere with 10 $^\circ\text{C}/\text{min}$ heating rate in the temperature range from 40 to 600 $^\circ\text{C}$. The dynamic mechanical stabilities of the hybrid membranes were evaluated by Mettler Toledo dynamic mechanical analyzer 861c instrument with Starc software under nitrogen with 10 $^\circ\text{C}/\text{min}$ heating rate in the temperature range 30- 300 $^\circ\text{C}$, to observe the effect of silica content on membrane mechanical stability. UV-DRS-diffuse reflectance spectra was obtained using Shimadzu(Model UV-DRS 2450). The optical densities of solutions were evaluated by using a VARIAN 50 bio UV-Vis spectrophotometer for adsorption studies.

4.7 ADSORPTION STUDIES

As already mentioned earlier in text crosslinked ZrTETA-55 hybrid chelating membrane exhibits strong interaction towards all metal ions, specially Cu^{2+} . Thus, all studies were performed using ZrTETA-55 chelating membrane. The effect of experimental conditions such as pH, adsorbate concentration, adsorption time, amount of adsorbent and temperature were studied to set the conditions for maximum

adsorption of the metal ion (Cu^{2+}) using ZrTETA-55 chelating membrane by batch process. In each experimental condition the amount of Cu^{2+} adsorbed by membrane was determined by following equation.

$$q = [(C_i - C_f)/1000 * W] * V \quad \text{(Eq. 4.16)}$$

where, q is the amount of Cu^{2+} adsorbed, C_i and C_f are the initial and final concentration ($\text{mg} \cdot \text{mL}^{-1}$) of Cu^{2+} before and after the adsorption, V is the volume of experimental solution, and W is the weight (g) of the membrane.

Effect of pH: Dry ZrTETA-55 membrane (0.5 g) was placed in a stoppered conical flask with 50 mL of Cu^{2+} solution of $50 \text{ mg} \cdot \text{L}^{-1}$ concentration, pH adjusted (using dilute HNO_3 and dilute NaOH in acid and alkaline range respectively), and the mixture shaken in a shaker incubator at 100 rpm for 30 min at room temperature (25°C). The concentration of Cu^{2+} in filtrate solution was determined using above equation (Eq. 4.16).

Effect of contact time: 50 mL of Cu^{2+} metal ion solution of concentration $50 \text{ mg} \cdot \text{L}^{-1}$ was equilibrated with 0.5 g ZrTETA-55 membrane in stoppered conical flasks for specific time intervals (100 – 800 min with increments of 100 min). In each case, the pH of the solution was adjusted to the value at which maximum sorption of Cu^{2+} takes place. After every prescribed time interval the amount of Cu^{2+} adsorbed was determined using above equation (Eq. 4.16).

Effect of concentration of Cu^{2+} : 0.5 g of dry ZrTETA-55 membrane was placed in a stoppered conical flask with 50 mL Cu^{2+} solution of varying concentrations ($50\text{-}200 \text{ mg} \cdot \text{L}^{-1}$ with $50 \text{ mg} \cdot \text{L}^{-1}$ increment) and mixture shaken in a shaker incubator at 100 rpm at optimized pH and optimum time at room temperature. The metal ion concentration was determined using equation (Eq. 4.16).

Effect of adsorbent dose: The effect of adsorbent dose was studied using 50 mL Cu^{2+} solution of ($50 \text{ mg} \cdot \text{L}^{-1}$) concentration, varying adsorbent dose from (0.1 to 1.0 g) at optimum pH, optimum time and at constant temperature, (25°C). In each case metal ion concentration was determined using equation (Eq. 4.16).

Effect of temperature: 50 mL of Cu^{2+} metal ion solution of concentration $50 \text{ mg} \cdot \text{L}^{-1}$ was equilibrated with 0.5 g of ZrTETA-55 membrane in stoppered conical flasks varying temperatures (298 K to 318 K with 10 K interval) and mixture shaken in a shaker incubator at 100 rpm at optimized time. The metal ion concentration was determined using equation (Eq. 4.16).

Thermodynamics: The adsorption process at varying temperature (298 K to 318 K with 10 K interval) was also used to evaluate the thermodynamic parameters such as free energy change (G°), enthalpy change (H°) and entropy change (S°) using equations [89].

$$K_c = C_{AC} / C_e \quad (\text{Eq. 4.17})$$

where K_c is the equilibrium constant, C_{AC} and C_e are equilibrium concentrations (mg.L^{-1}) of Cu^{2+} on ZrTETA-55 membrane and in the solution, respectively.

$$\Delta G^\circ = -2.303 RT \log K_C \quad (\text{Eq. 4.18})$$

where T is the absolute temperature (K) and R is the universal gas constant.

$$\log K_C = (\Delta S^\circ / 2.303 R) - (\Delta H^\circ / 2.303 RT) = \Delta G^\circ / RT \quad (\text{Eq. 4.19})$$

Kinetics: The rate constants were calculated using pseudo-first and second order kinetic models. The first order expression is given as,

$$\log(q_e - q) = \log q_e - \frac{K_1}{2.303t} \quad (\text{Eq. 4.20})$$

where q_e is the amount of Cu^{2+} adsorbed per unit weight of adsorbent at equilibrium or adsorption capacity (mg g^{-1}), and q the amount of Cu^{2+} adsorbed per unit weight of adsorbent at any given time t . K_1 is the first order rate constant and calculated from the slope of the linear plot of $\log(q_e - q)$ versus t at different Cu^{2+} initial concentrations. The kinetic rate equation for pseudo-second order is given as

$$\frac{t}{q} = \left(\frac{1}{h}\right) + \left(\frac{1}{q_e}\right)t \quad (\text{Eq. 4.21})$$

where, $h = K_2 q_e^2$ and K_2 is the rate constant of pseudo-second order adsorption ($\text{g mg}^{-1} \text{min}^{-1}$).

Adsorption isotherms: In the present study, the equilibrium data were derived from the linear form of Freundlich (Eq. 4.22) and Langmuir equation (Eq. 4.23) model of adsorption isotherms [90]:

$$\log q_e = \log K_F + 1/n (\log C_e) \quad (\text{Eq. 4.22})$$

$$C_e/q_e = 1/K_L + (a_L/K_L)C_e \quad (\text{Eq. 4.23})$$

where, C_e is the remaining Cu^{2+} ion concentration (mg.L^{-1}) in solution, q_e is the Cu^{2+} ion concentration (mg.g^{-1}) in the adsorbent, K_F is the Freundlich constant and $1/n$ is the heterogeneity factor, while a_L and K_L are the Langmuir constants.

The essential feature of Langmuir isotherm model can be expressed in terms of a dimensionless constant separation factor or equilibrium parameter (R_L) given by equation (Eq. 4.24)

$$R_L = 1/(1 + K_L * C_0) \quad \text{(Eq. 4.24)}$$

where K_L is the Langmuir constant and C_0 is the initial Cu^{2+} ion concentration (mg.L^{-1}).

Desorption studies: Desorption studies were performed by a batch process. 0.1 g of ZrTETA-55 membrane was treated with desired amount of adsorbent (Cu^{2+}) in a conical flask. Exchanged Cu^{2+} ZrTETA-55 membrane was now treated with 50 ml of each 0.1M HCl, 0.1 M HNO_3 , 0.1M NaCl, and 0.01M EDTA, separately for a fixed time (8h). The desorbed amount of Cu^{2+} was then determined by back titration using EDTA [91].

4.8 RESULTS AND DISCUSSION PART-I

Characterization of synthesized membrane

In chapter-III of the thesis details of nature of ZrT gel formation has been discussed in details and schematic structure of ZrT also presented in (Figure 3.21). FTIR spectrum exhibits broad band at $\sim 3400 \text{ cm}^{-1}$ attributed to symmetric and asymmetric $-\text{OH}$ stretching (Figure 4.4). Band at $\sim 1586 \text{ cm}^{-1}$ is attributed to C-C stretching vibration. Band at $\sim 1360 \text{ cm}^{-1}$ is assigned to C-N bending. No sharp bands for $-\text{OH}$ ($\sim 3400 \text{ cm}^{-1}$) and $-\text{NH}$ ($\sim 3300 \text{ cm}^{-1}$) stretching frequencies are observed probably due to merging of $-\text{OH}$ and $-\text{NH}$ group. A sharp medium band at $\sim 1642 \text{ cm}^{-1}$ ($\text{H}-\text{O}-\text{H}$ bending) confirms the presence of hydroxyl groups.

The ATR spectrum for cross-linked ZrTETA-55 membrane, exhibits bands at $\sim 1453 \text{ cm}^{-1}$ due to stretching vibrations of tertiary amines. A sharp band at $\sim 2353 \text{ cm}^{-1}$ confirms stretching of $\text{C}=\text{O}$ bond. The cross-linking is confirmed by the band at $\sim 1168 \text{ cm}^{-1}$ due to the $\text{C}-\text{O}-\text{C}$ alicyclic chain stretching vibration, which is absent for uncross-linked membrane.

^1H NMR spectrum for ZrTETA-55 membrane (Figure 4.5) shows peaks at $\delta 2.04$, $\delta 3.04$, $\delta 4.62$ and $\delta 5.62$ which interpret the presence of (multiplet, methylene $\text{CH}-\text{CH}_2-\text{CH}$), (multiplet, methylene $-\text{N}-\text{CH}_2-\text{CH}_2-\text{N}$), (multiplet, superimposed peak of methane and methylene, $\text{O}-\text{CH}$ and $\text{O}-\text{CH}_2$) and (singlet methylene and $\text{O}-\text{CH}_2-\text{O}$) respectively [92]. Based on the information obtained from FTIR studies and

¹H-NMR, schematic structure of ZrTETA-55 chelating membrane can be proposed as in **(Figure 4.6)**.

SEM image of ZrT particles exhibits amorphous nature with irregular particle size (rockshape) **(Figure 4.7)**. SEM micrographs **(Figures 4.8 and 4.9)** depicts surface and cross-section of ZrTETA-55 membrane, which indicate that inorganic precursor is homogeneously distributed at molecular level in organic matrix (PVA) without any clumps, clusters or agglomeration, due to inclusive interaction between the ZrT gel particles and the -OH groups of organic matrix (PVA).

DSC reveals **(Figure 4.10)** high T_g values for cross-linked membranes. With increasing ZrT gel content massive impact on T_g values were observed, due to profound ionic interactions via hydrogen bonding and compact polymer network. The mechanical strength of ZrTETA-X membranes also improved with increase in ZrT gel content **(Figure 4.11)**. ZrTETA-55 showed maximum stress capacity due to the stiffness provided by hydrogen bonding between -OH groups and thus adjusted polymer network formation [93].

Water Uptake and IEC

Membrane water uptake property affects conductivity, mechanical properties, and IUC etc. Water acts as carrier for counter-ion by vehicle mechanism and thus improves membrane conductivity [94]. But, excess of water uptake may result in undesirable dimensional augmentation, which ultimately leads to dimensional and mechanical instability. Water uptake (w) values for different ZrTETA-X membranes are presented in **(Table 4.2)**. With increase in precursor (ZrT) gel content, degree of cross-linking decreased, which further deteriorates membrane water uptake. Thus, water content was predominantly monitored by ZrT content in the membrane phase [95]. Furthermore, hydrophilic amino groups form large ionic clusters and accommodate large number of water molecules/ ionic site (w) [96]. Incorporation of ZrT gel in the membrane matrix enhanced the w values **(Table 4.2)**. Dimensional stability of ZrTETA-X membranes was examined by % swelling (w_{H_2O}) **(Table 4.2)**. Dimensional changes were isotropic in nature (almost similar in all directions) and increased with ZrT content in the membrane matrix.

IUC (defined as the number of ion uptake groups present in the polymer matrix), increased with ZrT gel content in the matrix **(Table 4.2)**. The IUC value of ZrTETA-55 was high (1.33 meq/g) compared to ZrTETA-45 membrane (0.46 meq/g).

IUC values were also used for the estimation of membrane void porosity (τ) and surface charge concentration (X^m) in the units of (moles of charge sites)/(cm³ of wet membrane) [96]. It is observed that surface charge concentration increased while membrane void porosity decreased with the increase in ZrT gel content in the membrane matrix (Table 4.2). Variation in membrane IUC values with ZrT gel content in the membrane matrix was responsible for increased surface charge concentration (Table 4.2), which facilitated the counter-ion conduction across the membrane.

Membrane Stability

Oxidative stability of ZrTETA-X membranes was assessed by treating membranes with Fenton's reagent for 3 h after which membrane weight was recorded [97,98]. ZrTETA-X membranes exhibited 4-6% weight loss under these experimental conditions. Further weight loss decreased with increasing ZrT gel content. Under these conditions membrane IUC loss was 2-3% (Table 4.3). These results revealed that oxidative degradation of cross-linked ZrTETA-X membranes took place on the main chain rather than functional groups. As a reference, Nafion117 membrane showed 5% weight loss under similar oxidative conditions [99]. Membrane hydrolytic stability was also examined by weight loss and IUC loss (Table 4.3). Membrane swelling was more prominent for membranes with low ionic domains (low ZrT gel content). Thus, membrane with low ZrT gel content exhibited more weight and IUC loss. These membranes were highly tolerant in nature in acidic condition (8.0 M HCl) and retained their properties with 2-7% swelling.

Metal ion adsorption on ZrTETA-55 membrane

To investigate the interaction of different metal ions, adsorption studies were performed in batch mode using ZrTETA-55, as a representative case. M²⁺ ion adsorption (%) was estimated by the ratio of amount of M²⁺ adsorbed and amount of M²⁺ taken for equilibration. ZrTETA-55 membrane showed relatively high adsorption for Cu²⁺ ion compared to other bi-valent metal ions (Ni²⁺, Zn²⁺, and Mn²⁺) (Figure 4.12).

Further, the UV-DRS spectrum for ZrTETA-55 membrane (Figure 4.13), before and after Cu²⁺ adsorption shows, there should be two types of Cu²⁺ isolated sites present in ZrTETA-55-Cu complex structure. Marison et al. [100] reported that the DRS peak ~620 nm is due to the bulk copper, while Cu²⁺ adsorbed ZrTETA-55

membrane exhibited peak around ~500 nm in this case. The peak in this region has been attributed to d-d transition band of a Cu^{2+} ion, centered in a pseudo-octahedral environment. Hence chelation of Cu^{2+} with active sites of ZrTETA-55 membrane occurred in pseudo-octahedral environment. Accordingly, structure of ZrTETA-55 membrane adsorbed with Cu^{2+} has been depicted in **(Figure 4.14)**.

WXR pattern **(Figure 4.15)** shows amorphous nature of pristine ZrTETA-55 as well as Cu^{2+} adsorbed ZrTETA-55 membrane, which was again confirmed by SEM image with irregular particle size. Further, EDX image of ZrTETA-55**(Figure 4.16)** and Cu^{2+} adsorbed ZrTETA-55 **(Figure 4.17)** membrane also revealed Cu^{2+} uptake by ZrTETA-55 membrane.

Membrane Conductivity, i - v Characteristics and Counter-Ion Transport Number :

Membrane conductivity data for ZrTETA-X membranes in equilibration with different metal salt solution (0.01M) followed the trend: $\text{Cu}^{2+} > \text{Ni}^{2+} > \text{Zn}^{2+} > \text{Mn}^{2+}$ **(Figure 4.18)**. Ionic mobility across the membrane channels reduced with increase in extent of hydration, which ultimately affected the membrane conductivity. Extent of hydration increases from Cu^{2+} - Ni^{2+} - Zn^{2+} - Mn^{2+} due to reduction in their ionic size, and thus conductivity also declines in the same trend [101, 102]. Membrane conductivity increases with increase in ZrT gel content in the membrane matrix. This observation may be attributed to the increase in IUC, water uptake, and hydrophilicity of the membrane matrix.

i - v curves for ZrTETA-X membranes in equilibration with NaCl solution (0.1 M) exhibit typical characteristic regions (Ohmic, non-Ohmic, and plateau) because of electro-migration of counter ions across the membrane, concentration polarization at membrane interface and water splitting **(Figure 4.19)** [99]. U_v , U_i , and I_{lim} values increased with ZrT gel content in the membrane matrix because of high counter-ion uptake in the membrane matrix **(Table 4.4)**. Thus, membrane with high ZrT gel content provides avenue for electro transport of counter-ions from the diffusive boundary layer to the membrane matrix, without any concentration polarization (I_{lim}). Counter-ions electro-transport through the membrane leads to concentration difference at membrane-solution interfacial zone and thus concentration polarization. Since, $t_i^m > t_i^s$ (counter-ion transport number in solution), their flux in the membrane ($J_i^m = t_i^m I / F_{zi}$) is always larger than in the boundary layer because t_i^m is

proportional to (j_i^m) . Thus, values of I_{lim} depend on boundary layer thickness, t_i^m and electrolyte environment. ZrTETA-55 membrane showed excellent electro-transport properties and may be used for the practical separation of metal ions. Also, studies on *i-v* curves are quite useful for forecasting the suitability of given membranes for utilization in separation processes [16].

The t_i^m values were estimated by Hittorf's method for different counter-ions across ZrTETA-X membranes (**Figure 4.20**), and depends on nature of counter-ions and membrane matrix. t_i^m values increased with ZrT gel content in membrane matrix. Low Donnan exclusion due to low surface charge density was attributed for relatively low t_i^m values. Counter-ion transport number of different bi-valent ions followed the trend ($\text{Cu}^{2+} > \text{Ni}^{2+} > \text{Zn}^{2+} > \text{Mn}^{2+}$) for ZrTETA-X membranes. In case of different counter-ions, transport number also depends on their affinity with membrane interface, membrane pore size and radius of the hydrated ions.

Electro Osmotic Permeability Studies:

To study the electro-transport of solvent/water across the ZrTETA-X membranes, electro-osmotic permeability values were measured and electro-osmotic flux vs applied voltage data presented in (**Figure 4.21**).

Equivalent pore radii (r) for different ZrTETA-X membranes was estimated from Katchalsky and Curran approach [103], by estimating necessary coulomb of electricity required to exert a desired drag (cm^3) through 1 cm^2 of the membrane area. Equivalent pore radius increased with ZrT gel content in the membrane matrix (**Table 4.2**), which may be attributed to the integration of functional/hydrophilic groups in the membrane matrix leading to enhanced hydrophilic domains and pore radius. Membrane pore radius data indicated that the membranes were quite dense in nature (5-16 Å) and can be efficiently used in electro-transport processes.

Electro-Dialytic Separation of Copper ion:

ED stack with five compartments (schematically depicted in **Figure 4.2**) was employed to achieve the selective separation of Cu^{2+} from other bi-valent cations (Cu^{2+} , Ni^{2+} , Zn^{2+} , Mn^{2+}) under constant applied current (10 mA cm^{-2}). Na_2SO_4 solution (0.1M) was used as electrode wash, while desired electrolytic solutions ($\text{M}_2(\text{SO}_4)$) (separately or mixed) were fed into compartments 1 and 3. Electro-transport of different metal ions, from compartments 1 and 3 to compartment 2, was

monitored by either their concentration depletion in previous or concentration build-up in latter. With onset of the experiments, concentration changes in output streams were recorded as function of time, for estimating rate of metal ion transport (flux). Electro-transport flux for metal ions (J) from compartment 1 and 3 to compartment 2 may be obtained by the following relation, considering negligible mass (water) transport through membranes,

$$J = \frac{V_a (\Delta C)}{A \Delta t} \quad \text{(Eq. 4.17)}$$

where C is the change in Cu^{2+} concentration (initial and final (mol m^{-3})); t is the time allowed for the process (s); V_a is the total volume of feed in each stream ($5.0 \times 10^{-4} \text{ m}^3$); and A is the effective membrane area ($8.0 \times 10^{-3} \text{ m}^2$). Flux of different bi-valent metal ions across ZrTETA-X membranes at 10.0 mA cm^{-2} were compared (**Figure 4.22**). ZrTETA-X membranes exhibited comparatively very high flux for Cu^{2+} in comparison to other bi-valent metal ions. Furthermore, flux values for different metal ions across ZrTETA-X membranes followed the trend: $\text{Cu}^{2+} > \text{Ni}^{2+} > \text{Zn}^{2+} > \text{Mn}^{2+}$, which is similar to its counter-ion transport number in the membrane matrix (**Figure 4.23**) and adsorption capacity on ZrTETA-55 membrane (**Figure 4.12**). Accountable features for pronounced selectivity for Cu^{2+} across the ZrTETA-X membranes are cross-linked structure and formation of chelates with membrane matrix. Selective electro-transport of Cu^{2+} across ZrTETA-X membranes in presence of other bi-valent metal ions occurs in three steps: selective adsorption of Cu^{2+} at interface of ZrTETA-X membranes and formation of chelates; electro-assisted diffusion of Cu^{2+} across the ZrTETA-X membranes towards cathode (on the principle electrodialysis); desorption of Cu^{2+} at other surface on ZrTETA-X membranes and salt formation. In this case, it is interesting to record that Cu^{2+} selectively adsorbed on the membrane surface and formed chelates in pseudo-octahedral environment with ZrTETA-X membranes.

Rate of equilibrium between the chelating groups on the membrane matrix depends on the size of exchanging ion and ability of dissociation of fixed charge from the membrane matrix. Metal cations have hydration tendency, depending on their ion size. Relatively larger ions are less hydrated, thus less hydration energy is required for dehydration to occupy an exchangeable site. This phenomenon also plays a prominent role, while determining selectivity. Considering the ionic size for different bi-valent metal ions ($\text{Cu}^{2+}(0.69\text{\AA}) > \text{Ni}^{2+}(0.72\text{\AA}) > \text{Zn}^{2+}(0.74\text{\AA}) > \text{Mn}^{2+}(0.80\text{\AA})$), comparatively

high selectivity for Cu^{2+} also can be concluded. Also, among prepared ZrTETA-X membranes, ZrTETA-55 showed the highest flux values, which may be attributed to high chelating sites and surface charge density. Interestingly, during course of investigation no membrane fouling or deterioration in the membrane performance was observed.

Electrodialysis experiments with equi-molar metal ion solution mixtures (0.10 M) at 10 mA cm^{-2} applied current density, using different ZrTETA-X chelating membranes were conducted, to observe the feasibility for electro-separation/recovery of Cu^{2+} from other bi-valent metal cations. Separation factor (SF) was estimated from the ratio of Cu^{2+} flux with other bi-valent cation flux ($J_{\text{Cu}^{2+}}/J_{\text{M}^{2+}}$) in case of bi-valent metal ions mixture and taken as advantage to assess the suitability of different ZrTETA-X chelating membranes for separating Cu^{2+} . ZrTETA-55 membrane showed 3.75 SF value for $\text{Cu}^{2+}/\text{Ni}^{2+}$, while 3.22 and 3.01 SF values for $\text{Cu}^{2+}/\text{Zn}^{2+}$ and $\text{Cu}^{2+}/\text{Mn}^{2+}$, respectively (**Figure 4.24**). ZrTETA-X membranes have the special structural characteristics, in which Cu^{2+} is electro-transported through the hydrophilic channels containing amino groups, while it was not suitable for other bi-valent cations. Reported membrane exhibited high selectivity for Cu^{2+} , suitable for electro-separation of Cu^{2+} in presence of other bi-valent metal ions. Highly cross-linked and hydrophilic structural membrane morphology, presence of plenty of amino groups able to form chelates with Cu^{2+} are the responsible factors for governing specific membrane selectivity. As a reference, selectivity factor values for Cu^{2+} and different metal cations were also determined for commercial Nafion membrane. For this, ZrTETA-X membrane in ED unit (**Figure 4.2**) was replaced by Nafion membrane of similar dimension. Interestingly, Nafion membrane did not show any selective separation between metal cations. Further, SF values for Cu^{2+} with different metal cations were close to unity (**Figure 4.24**).

The smart features of the ZrTETA-X membranes are its simple and eco-friendly preparation methodology, high specific selectivity, and stabilities (thermal, mechanical and chemical). Furthermore, ZrTETA-X membranes in combination with electrodialysis offer valuable option for separation/recovery of Cu^{2+} from other bi-valent metal ions from industrial waste waters.

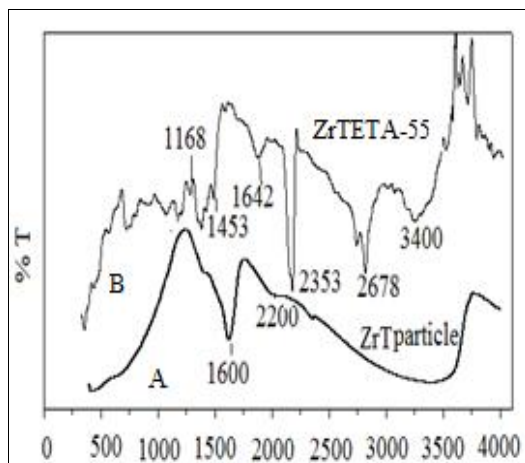


Figure 4.4 ATR Spectra of (A) ZrT particle (B) Cross linked ZrTETA-55 membrane

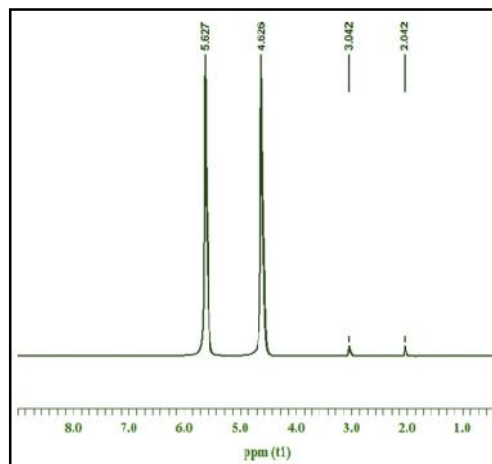


Figure 4.5 ¹H-NMR spectrum of ZrTETA-55 membrane

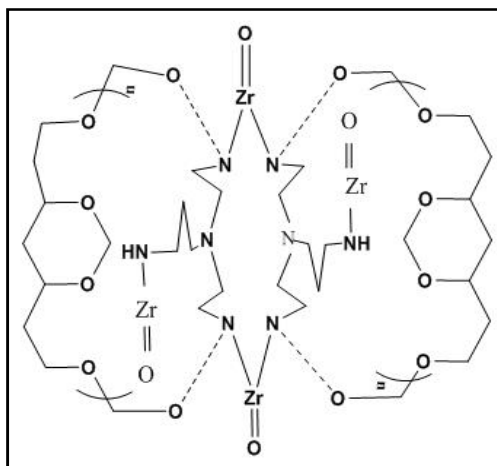


Figure 4.6 Schematic structure of ZrTETA-55 membrane

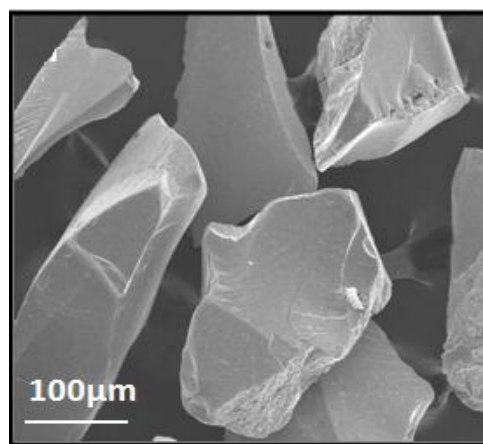


Figure 4.7 SEM images of ZrT gel particles

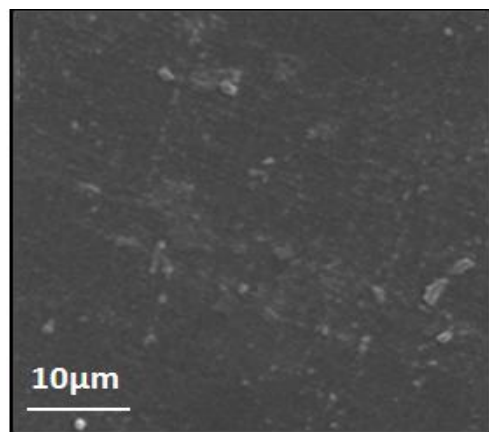


Figure 4.8 SEM image of surface of ZrTETA-55 membrane

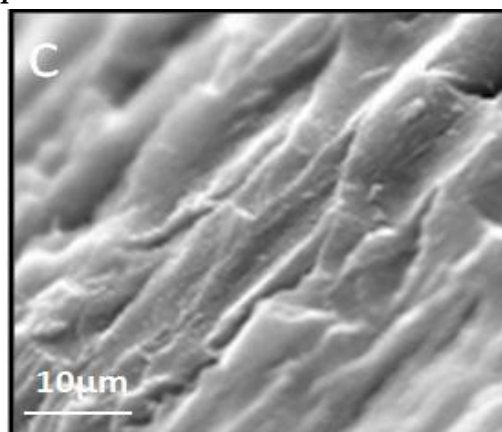


Figure 4.9 SEM image of cross section of ZrTETA-55 membrane

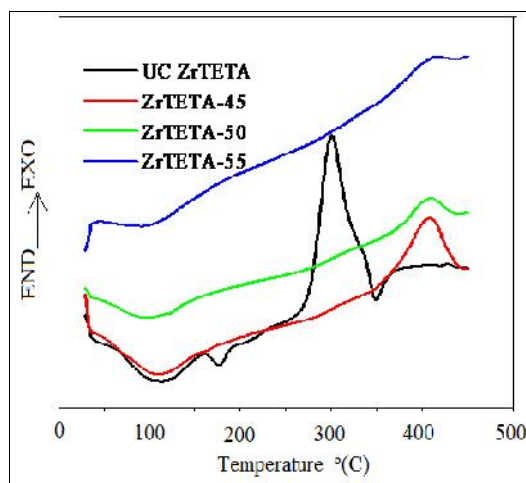


Figure 4.10 DSC of ZrTETA-X membranes

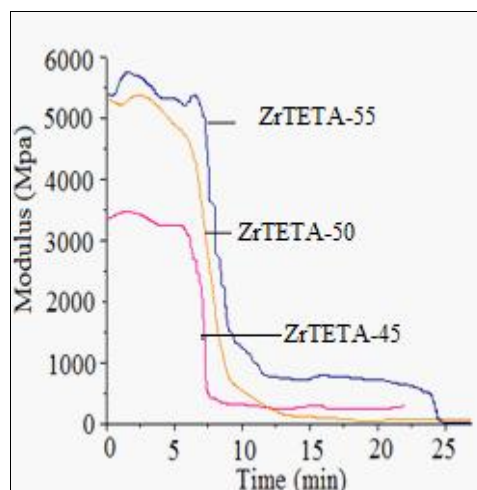


Figure 4.11 DMA curves for ZrTETA-X membranes

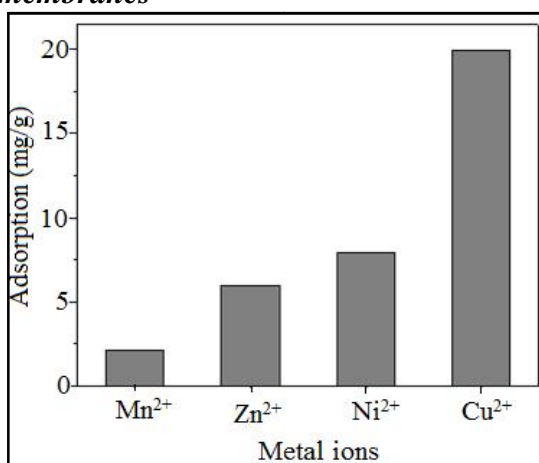


Figure 4.12 Adsorption capacity of ZrTETA-55 membrane for different metal ions

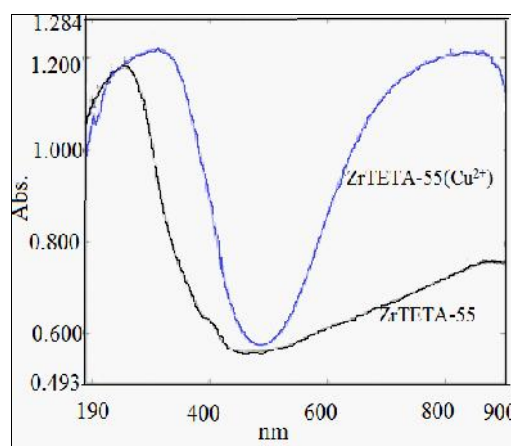


Figure 4.13 Diffuse reflectance spectrum (DRS) for ZrTETA-55 membrane before and after Cu²⁺ chelation

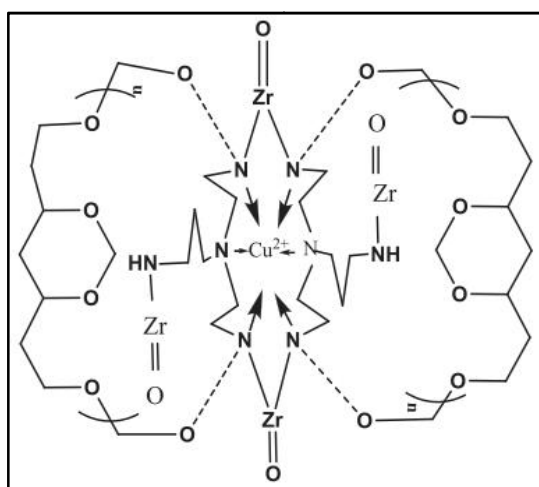


Figure 4.14 Proposed structure for Cu²⁺ chelated ZrTETA-55 membrane

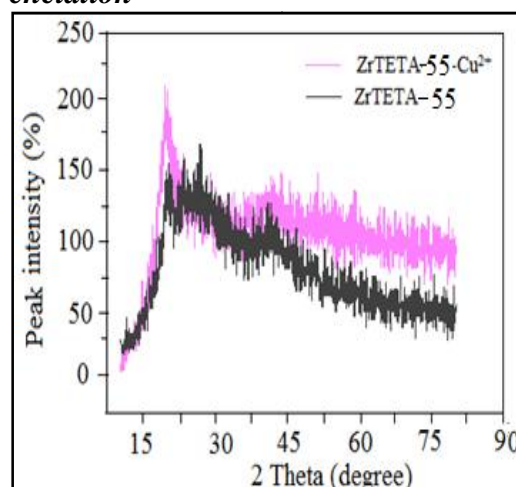


Figure 4.15 WXR D pattern of ZrTETA-55 and Cu²⁺ Chelated ZrTETA-55 membrane

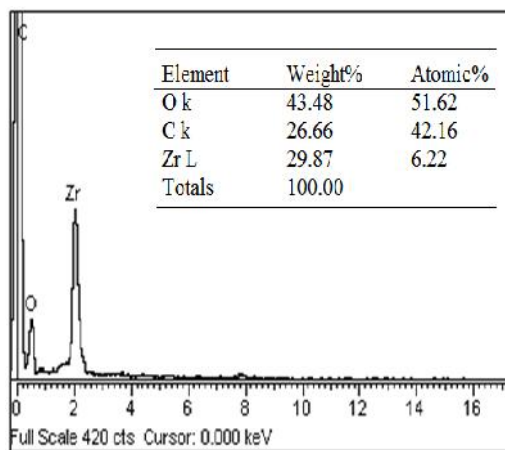


Figure 4.16 EDX of ZrTETA-55 membrane

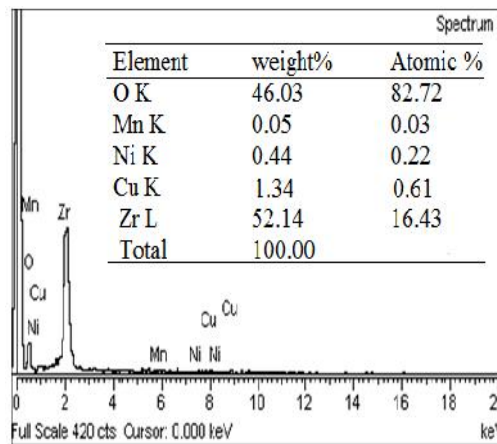


Figure 4.17 EDX of Cu²⁺ chelated ZrTETA-55 membrane

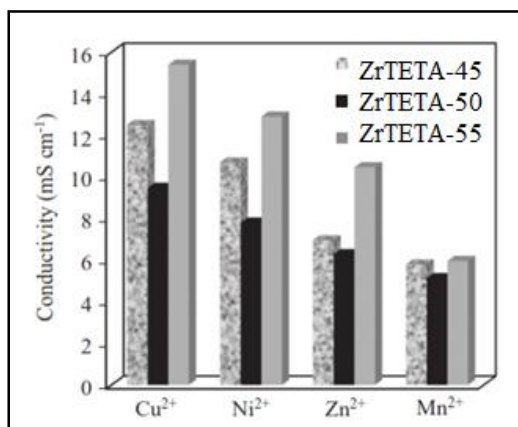


Figure 4.18 Membrane conductivity data in equilibration of different metal salt solutions (0.01 M)

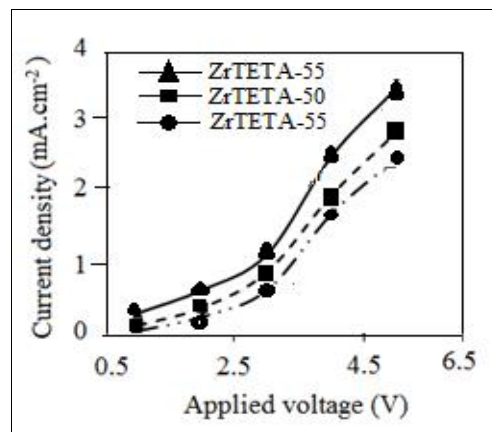


Figure 4.19 *i-v* characteristics for ZrTETA-*X* membranes in equilibration with 0.10M NaCl solution

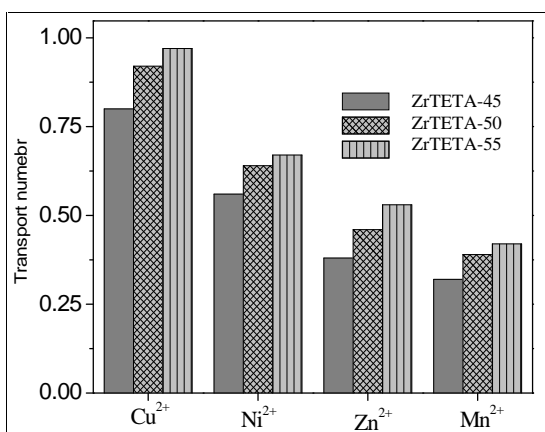


Figure 4.20 t_i^m values in equilibration with 0.1M metal ion solutions across ZrTETA-*X* membranes

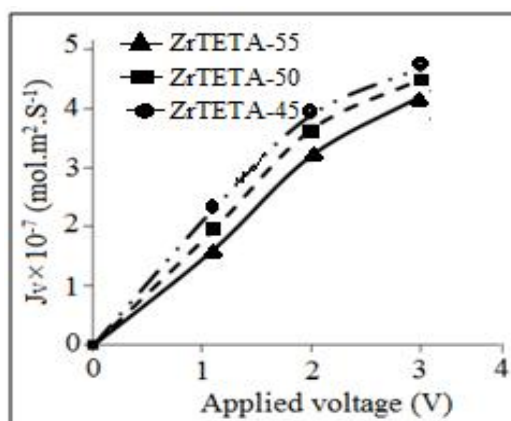


Figure 4.21 Variation of electro osmotic flux (J_v) with applied voltage for different ZrTETA-*X* membranes

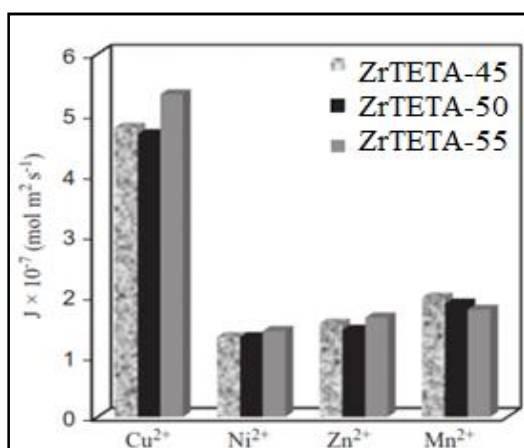


Figure 4.22 Electro-transport flux for different metal ions (J) (0.10 M) across ZrTETA-X membranes at 10 mA/cm² applied current density

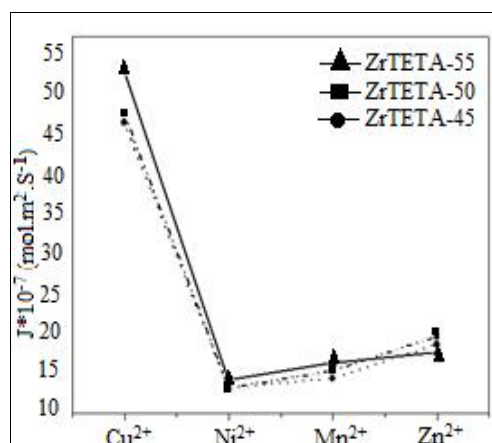


Figure 4.23 Ionic flux data across different ZrTETA-X membranes for various metal ions (0.10M) under 10 mA/cm² applied current density

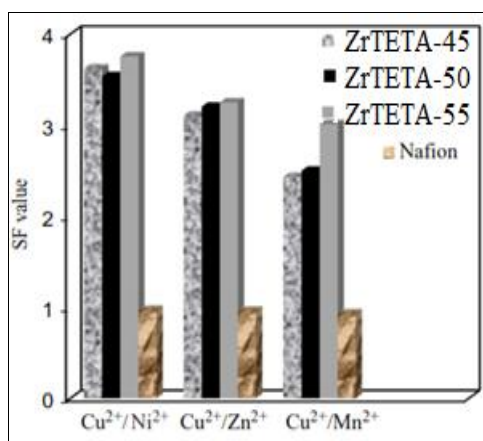


Figure 4.24 Separation factor (SF) of different equi-molar metal ion mixtures (0.10 M) for ZrTETA-X membranes under 10 mA/cm² applied current density

Table 4.2 w , H_2O , IUC , $r(\text{Å})$, X_m , and w values for different ZrTETA-X membranes

| Membrane | $w(\%)$ | $H_2O(\%)$ | $IUC(\text{meq}\cdot\text{g}^{-1})$ | $r(\text{Å})$ | $X_m(\text{mmoldm}^{-3})$ | w |
|-----------|---------|------------|-------------------------------------|---------------|---------------------------|-------|
| ZrTETA-45 | 22.6 | 12.14 | 0.46 | 5.39 | 0.53 | 5.91 |
| ZrTETA-50 | 25.45 | 19.23 | 0.47 | 11.87 | 0.85 | 9.26 |
| ZrTETA-55 | 27.25 | 21.18 | 1.33 | 16.24 | 1.89 | 28.64 |

Table 4.3 Oxidative and Hydrolytic Stabilities for ZrTETA-X Chelating Membranes

| Membrane | Oxidative Stability | | Hydrolytic Stability | |
|-----------|---------------------|--------------|----------------------|--------------|
| | Weight Loss (%) | IUC Loss (%) | Weight Loss (%) | IUC Loss (%) |
| ZrTETA-45 | 5.49 | 3.06 | 1.28 | 1.32 |
| ZrTETA-50 | 5.42 | 2.74 | 1.04 | 1.01 |
| ZrTETA-55 | 4.20 | 2.58 | 1.02 | 0.94 |

Table 4.4 Characteristic values of i - v curves for ZrTETA-X membranes in equilibration with 0.10 M NaCl solutions

| Membrane | $V(\text{Volt})$ | $I(\text{mA}/\text{cm}^2)$ | $I_{lim}(\text{mA}/\text{cm}^2)$ |
|-----------|------------------|----------------------------|----------------------------------|
| ZrTETA-45 | 1.704 | 0.981 | 1.3 |
| ZrTETA-50 | 1.921 | 1.342 | 1.78 |
| ZrTETA-55 | 1.924 | 1.823 | 2.5 |

4.9 RESULTS AND DISCUSSION PART-II

Amongst the chelating membranes prepared of varying gel composition, crosslinked ZrTETA-55 hybrid chelating membrane exhibits strong interaction towards all metal ions, specially Cu^{2+} . Thus, thermodynamic, kinetic and adsorption studies were performed using ZrTETA-55 chelating membrane which involves effect of time, temperature, pH, adsorbent dose, and adsorbate concentration, towards adsorption of Cu^{2+} . Pseudo-first and pseudo second order kinetic models, thermodynamic parameters {(Standard free energy (UG°), enthalpy (UH°) and entropy (US°)} have been evaluated and adsorption isotherms (Langmuir and Freundlich) studied.

Effect of pH

The effect of pH on adsorption of Cu^{2+} ion was studied in pH range (2-12) (**Figure 4.25**). Amount of Cu^{2+} adsorbed at pH: 2 was observed to be about 44%, which further increased and attained a maximum value of 73.75% at pH 6.0. In acidic medium ($\text{pH} < 7$) due to high H^+ ion concentration, active sites of the adsorbent being protonated probably reduces Cu^{2+} adsorption [104]. With increase in pH, deprotonation of amino groups enhances adsorption of Cu^{2+} . The solubility of metals decreases with increasing pH, and metal hydroxides precipitate on the surface of adsorbent. At a constant concentration, the adsorption capacity increases with solution pH and attains a limiting value beyond pH: 7.0. The precipitation of Cu^{2+} as hydroxide was found to occur in basic solution, therefore all adsorption studies were carried out in low acidic medium at pH: 7.0.

Effect of contact time

The effect of contact time on the adsorption of Cu^{2+} at different concentrations is presented in (**Figure 4.26**). Initially, rate of adsorption is faster upto 6h and maximum removal of Cu^{2+} is observed. Thus, all further experiments were performed after allowing an 8h equilibrium time. In the beginning fast adsorption, is explained due to the availability of more number of adsorption sites [105, 106]. Subsequently availability of adsorption sites decrease and thus rate of adsorption decreases [107].

Effect of concentration of Cu²⁺

Effect of concentration on Cu²⁺ adsorption was studied in concentration range (50-200 mg.L⁻¹). It is observed that at low Cu²⁺ concentration, close to 97.5 % adsorption was observed (**Figure 4.27**). At 50 mg.L⁻¹ Cu²⁺ concentration, about 74% adsorption was observed, which further reduced steeply with Cu²⁺ concentration up to 200 mg. L⁻¹. These data can be used effectively to ascertain the maximum utilization of adsorbent for Cu²⁺ separation. High adsorption (close to 97%) of Cu²⁺ by ZrTETA-55 hybrid membrane confirmed its potential application for selective separation of Cu²⁺ in the presence of other bi-valent metal ions. Furthermore, to optimize the dose of adsorbent, concentration of adsorbate for selective separation of Cu²⁺ is necessary to achieve maximum performance.

Effect of adsorbent dose

The plots of initial Cu²⁺ concentration, vs adsorbent dose (0.1-1.0g) at constant temperature (25 °C) is presented in (**Figure 4.28**). Adsorption (%) increased from 27.5 to 78 % while adsorption density decreased from 39.43 to 13.97 mg.g⁻¹ with the increase in adsorbent dose. The reduction in adsorption density may be due to the fact that some of the adsorption sites remain unsaturated when adsorbent dose is increased. On the other hand large amount of Cu²⁺ was adsorbed as the number of available adsorption sites are increased, resulting in overall increase in the removal efficiency [108].

Effect of temperature and evaluation of thermodynamic parameters

Various thermodynamic parameters such as, standard Gibbs free energy (G°), enthalpy (H°) and entropy (S°) have been evaluated using standard equations (**Eq. 4.17-4.19**) discussed earlier in text and results presented in (**Table 4.5**).

The values of ΔH° and ΔS° were calculated from the slope and intercept of Vant Hoff plot ($\log K_c$ versus $1/T$ in **Figure 4.29**) and data presented in (**Table 4.5**). It is observed that UH° and US° increased with temperature, while UG° decreased. Thus the Cu²⁺ adsorption on crosslinked ZrTETA-55 hybrid membrane is endothermic in nature [109]. It was further observed that the Cu²⁺ adsorption is spontaneous and spontaneity increased with the temperature. Positive value of US° suggests randomness at the solid-solution interface during adsorption [110].

Adsorption mechanism and kinetics

The pseudo- first order and pseudo-second order rate constants and correlation coefficients were evaluated using equations (Eq. 4.20 and 4.21). Pseudo-first order constant (K_1) correlation coefficient (R^2) were calculated from plots $\log(q-q_e)$ versus t (min) (Figure 4.30) and values presented in (Table 4.6). Pseudo-second order constant K_2 , h and R^2 were calculated from the intercept of the linear plots of t/q versus t (Figure 4.31) values presented in (Table 4.6). These data show that adsorption process of Cu^{2+} on ZrTETA-55 membrane followed second order kinetics under studied concentration range (25-100 mg. L⁻¹), rather than pseudo-first order kinetics [111]. The experimentally calculated values of q_e at various Cu^{2+} concentrations were in good agreement with theoretical calculated values. Furthermore, the values of correlation coefficients (R^2) for pseudo-first-order kinetic model are slightly lower than the pseudo-second-order kinetic model, indicating that pseudo second order kinetic model is better obeyed in comparison with the pseudo-first-order kinetic model.

Adsorption isotherms

The Langmuir and Freundlich constants were calculated from the plots of C_e/q_e vs C_e and $\log q_e$ vs $\log C_e$ respectively. Various constants and R^2 for Freundlich isotherm are presented in (Table 4.7) and (Figure 4.32). Data showed the deviation from linearity (total concentration range is taken into consideration). This may be due to either: (i) the presence of different groups such as amino, hydroxyl, acetyl in the crosslinked ZrTETA-55 membrane producing irregular energy distribution in the adsorbent, or (ii) by a purely physical adsorption [107,112]. However, Langmuir isotherm model correlated well ($R^2 = 0.999$) as compared to Freundlich isotherm ($R^2 = 0.995$) only, when one line was used to represent the entire range of experimental data as shown in (Figure 4.33). The values of Langmuir constants and (R^2) are derived from the linear curves of Langmuir isotherm and the values reported in (Table 4.7). It is concluded that the values of a_L increased with temperature, which indicated the strong binding of Cu^{2+} ion with $-\text{NH}_2$ group. It was also found that the monolayer saturation capacity (Q_0) values increased with temperature. Experimental findings are also well correlated with the saturation capacities, predicted by Langmuir equation at different temperatures.

R_L values have been calculated for varying temperatures (298K, 308K, 318K) and varying concentration of Cu^{2+} ion (25, 50, 75, 100 mg.L^{-1}) (**Table 4.8**). It is observed that for each concentration of Cu^{2+} studied, the R_L values decrease with increase in temperature. Further, for each temperature studied, R_L values decrease with increase in concentration. It is concluded that at 298 K and 25mg.L^{-1} Cu^{2+} concentration R_L values are highest indicating favorable adsorption. [113].

Desorption study

Desorption studies help to reveal the nature of adsorption process and to recover the Cu^{2+} ions from cross-linked ZrTETA-55. Desorption studies were carried out by using HCl, NaOH, HNO_3 , NaCl and EDTA solution. Around 62-90 % recovery of Cu^{2+} was observed on desorption studies, with almost 90% of Cu^{2+} ion recovery using 0.1 M HCl and 62.4 % using 0.01M EDTA.

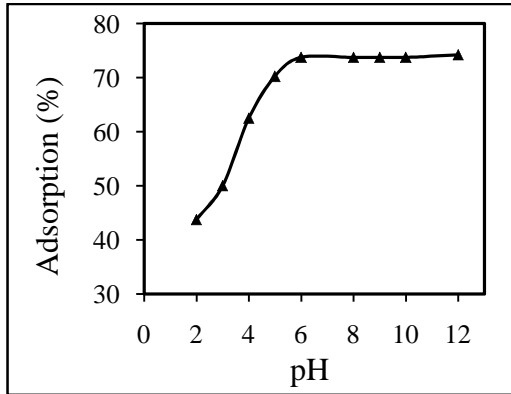


Figure 4.25 Effect of pH on Cu^{2+} adsorption towards crosslinked ZrTETA-55 hybrid membrane

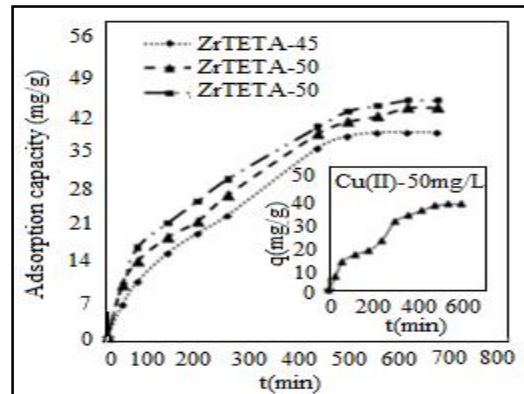


Figure 4.26 Effect of contact time on the adsorption of Cu^{2+} at different concentrations using ZrTETA-55 hybrid membrane

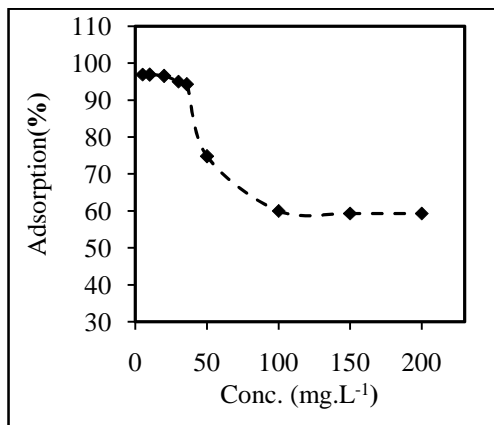


Figure 4.27 Effect of Cu^{2+} concentration on adsorption (%) using crosslinked ZrTETA-55 hybrid membrane at pH 7.0

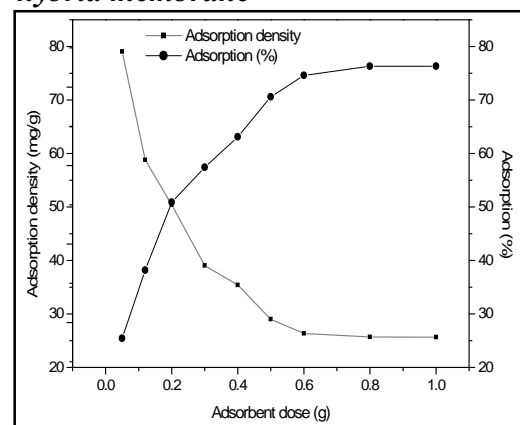


Figure 4.28 Effect of adsorbent dose for Cu^{2+} (50mg.L^{-1}) adsorption using crosslinked ZrTETA-55 hybrid membrane

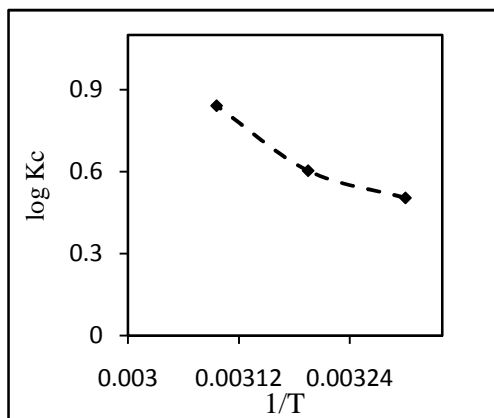


Figure 4.29 Vant Hoff plot [$\log K_c$ vs. $1/T$]

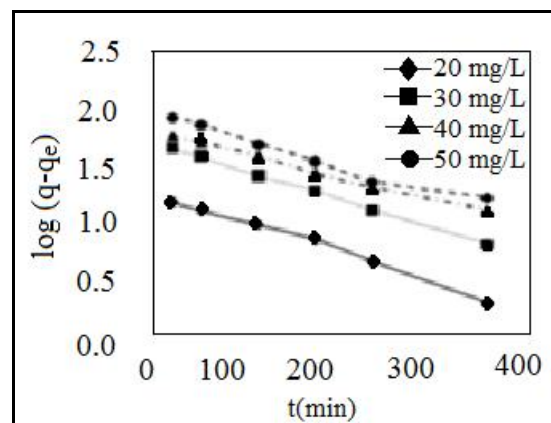


Figure 4.30 Pseudo first order plots for Cu^{2+} adsorption on crosslinked ZrTETA-55 hybrid membrane at different concentration

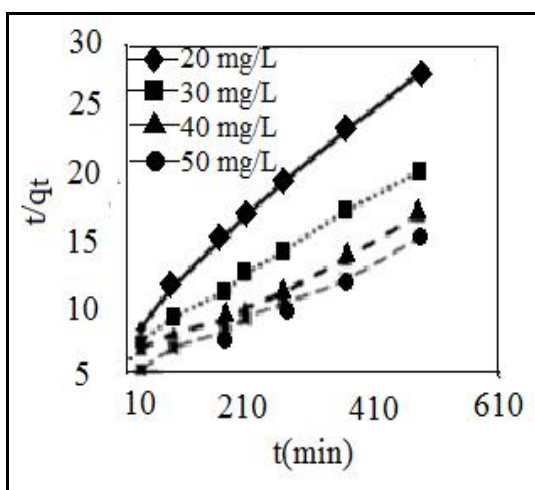


Figure 4.31 Pseudo second order plot for Cu^{2+} adsorption on crosslinked ZrTETA-55 hybrid membrane at different concentration (pH 7.0)

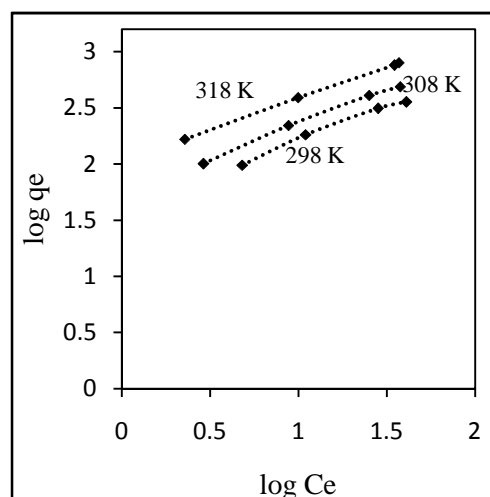


Figure 4.32 Freundlich plots for Cu^{2+} adsorption on crosslinked ZrTETA-55 hybrid membrane under different experimental conditions

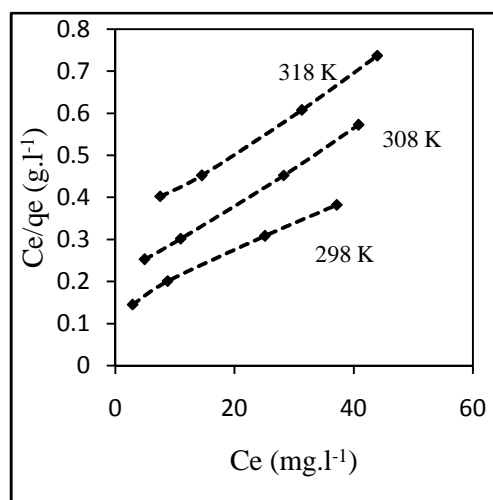


Figure 4.33 Langmuir plot for Cu^{2+} adsorption on crosslinked ZrTETA-55 hybrid membrane under different experimental conditions

Table 4.5 Thermodynamic parameters and correlation coefficients (R^2) at different temperatures for the adsorption of Cu^{2+} on crosslinked ZrTETA-55 hybrid membrane at pH 7.0

| Temperature (K) | US' (kJ K ⁻¹ mol ⁻¹) | UH' (kJ mol ⁻¹) | UG' (kJ mol ⁻¹) | R ² |
|-----------------|---|-----------------------------|-----------------------------|----------------|
| 298 | 0.11 | 28.02 | -2.71 | -- |
| 308 | 0.12 | 33.31 | -4.1 | 0.99 |
| 318 | 0.15 | 39.69 | -5.30 | -- |

Deviation in R² values = ± 0.02 Deviation in US' = ± 0.01, Deviation in UH' and UG' = ± 1,

Table 4.6 Pseudo-first- and second-order kinetic constants and correlation coefficients (R^2) for Cu^{2+} adsorption at pH 7.0 using ZrTETA-55 hybrid membrane

| Concentration of Cu ²⁺ (mg L ⁻¹) | Pseudo-first-order Kinetics | | Pseudo-second-order kinetics | | | |
|---|-------------------------------------|----------------|--|--------------------------------------|-------------------------|----------------|
| | K ₁ (min ⁻¹) | R ² | K ₂ (g mg ⁻¹ min ⁻¹) | q _e (mg g ⁻¹) | h (mg g ⁻¹) | R ² |
| 25 | 0.00599 | 0.986 | 0.000123 | 27.71 | 0.0899 | 0.9967 |
| 50 | 0.00575 | 0.996 | 0.000115 | 31.64 | 0.1057 | 0.9977 |
| 100 | 0.00483 | 0.993 | 0.000110 | 50.61 | 0.1512 | 0.995 |

Deviation in R² values = ± 0.005

Table 4.7 Freundlich and Langmuir constants and correlation coefficients (R^2) for Cu^{2+} adsorption on ZrTETA-55 hybrid membrane at pH 7.0

| Temperature (K) | Freundlich constants | | | | Langmuir constants | | | |
|-----------------|----------------------|--------|------|----------------|--------------------|----------------|--------------------------------------|----------------|
| | K _F | 1/n | n | R ² | K _L | a _L | Q _o (mg g ⁻¹) | R ² |
| 298 | 22.06 | 0.6896 | 1.49 | 0.98 | 3.09 | 0.027 | 105.14 | 0.992 |
| 308 | 37.38 | 0.6134 | 1.59 | 0.98 | 5.32 | 0.051 | 110.13 | 0.998 |
| 318 | 53.55 | 0.6172 | 1.60 | 0.99 | 7.56 | 0.052 | 141.9 | 0.996 |

Deviation in K_F and K_L values = ± 2, Deviation in R² values = ± 0.005

Table 4.8 Langmuir correlation coefficients (R_L) for Cu^{2+} adsorption at different concentration on ZrTETA-55 hybrid membrane at pH 7.0

| Temperature (K) | 25 (mg. L ⁻¹) | 50 (mg. L ⁻¹) | 75 (mg. L ⁻¹) | 100 (mg.L ⁻¹) |
|-----------------|---------------------------|---------------------------|---------------------------|---------------------------|
| 298 | 0.587 | 0.420 | 0.407 | 0.271 |
| 308 | 0.486 | 0.320 | 0.251 | 0.190 |
| 318 | 0.451 | 0.290 | 0.212 | 0.165 |

Deviation in R_L values = ± 0.005

4.10 CONCLUSIONS

Prepared ZrTETA-X chelating membranes exhibited high thermal, mechanical and chemical stabilities along with good IUC and conductivity. Counter-ion transport number in the membrane phase and $i-v$ characteristics of ZrTETA-X membranes suggested their specific selectivity for Cu^{2+} in comparison with other bi-valent metal cations. Adsorption studies confirmed very high uptake for Cu^{2+} in comparison to other bi-valent metal ions (Ni^{2+} , Zn^{2+} , and Mn^{2+}). Electro-dialytic separation studies of bi-valent metal cations also confirmed very high flux for Cu^{2+} in comparison to other cations. Moreover, high separation factor (3.0–4.0) for separating $\text{Cu}^{2+}/\text{Ni}^{2+}$, $\text{Cu}^{2+}/\text{Mn}^{2+}$ and $\text{Cu}^{2+}/\text{Mn}^{2+}$, suggested practical applications of developed membrane for selective separation/recovery of Cu^{2+} from industrial waste water.

UH° and US° values increased with temperature, while UG° values decreased. Thus, the Cu^{2+} adsorption on crosslinked ZrTETA-55 hybrid membrane is endothermic in nature. It was further observed that the Cu^{2+} adsorption is spontaneous and spontaneity increased with the temperature. Positive value of US° suggests randomness at the solid-solution interface during adsorption.

Adsorption process of Cu^{2+} on ZrTETA-55 membrane followed second order kinetics under studied concentration range (25-100 mg.L^{-1}). Further, the values of correlation coefficients (R^2) for pseudo-first-order kinetic model are slightly lower than the pseudo-second-order kinetic model, indicating that pseudo second order kinetic model is better obeyed in comparison with the pseudo-first-order kinetic model. Based on a linearized correlation coefficient, the Langmuir isotherm model gives better fit than the Freundlich isotherm model.

REFERENCE

- [1] Strathman H, Electrodialysis and related processes. In: Noble R D, Stern S A, (editors) *Membrane separation technology. Principles and applications*. Elsevier Science B.V. (1995) 213-223.
- [2] Park J S, Chilcott T C, Coster H G L, Moon S H, *Characterization of BSA-fouling of ion-exchange membrane systems using a subtraction technique for lumped data*, **J Membr Sci**, 246 (2005) 137-144.
- [3] Gartner R S, Wilhelm F G, Witkamp G J, Wessling M. *Regeneration of mixed solvent by electrodialysis: selective removal of chloride and sulfate*, **J Membr Sci**, 250 (2005) 113-133.
- [4] Choi J H, Moon S H, *Pore size characterization of cation-exchange membranes by chronopotentiometry using homologous amine ions*, **J Membr Sci**, 191 (2001) 225-236.
- [5] Lebrun L, Follain N, Metayer M, *Pore size characterization of cation-exchange membranes by chronopotentiometry using homologous amine ions*, **Electrochim Acta**, 50 (2004) 985-993.
- [6] Tongwen X, Weihua Y, *Fundamental studies of a new series of anion exchange membranes: membrane preparation and characterization*, **J Membr Sci**, 190 (2001) 159-166.
- [7] Nagarale R K, Gohil G S, Shahi V K, *Recent developments on ion-exchange membranes and electro-membrane processes*, **Adv Colloid Interface Sci**, 119 (2006) 97-130.
- [8] Nagarale R K, Shahi V K, Rangarajan R, *Preparation of polyvinyl alcohol-silica hybrid heterogeneous anion-exchange membranes by sol-gel method and their characterization*, **J Membr Sci**, 248 (2005) 37-44.
- [9] Hench L L, West J K, *The sol-gel process*, **Chem Rev**, 90 (1990) 33-72.
- [10] Kurumada K, Nakabayashi H, Murataki T, Tanigali M, *Structure and formation process of silica microparticles and monolithic gels prepared by the sol-gel method*, **Collo Surf A Physicochem Eng Asp**, 139 (1998) 163-170.
- [11] Nagarale R K, Gohil G S, Shahi V K, Rangarajan R, *Organic–Inorganic Hybrid Membrane: Thermally Stable Cation-Exchange Membrane Prepared by the Sol–Gel Method*, **Macromolecules**, 37 (2004) 10023-10030.

- [12] Kim D S, Park H B, Rhim J W, Lee Y M, *Preparation and characterization of crosslinked PVA/SiO₂ hybrid membranes containing sulfonic acid groups for direct methanol fuel cell applications*, **J Membr Sci**, 240 (2004) 37-48.
- [13] Mutin P H, Guerrero G, Vioux A, *Organic-inorganic hybrid materials based on organophosphorus coupling molecules: from metal phosphonates to surface modification of oxides*, **C R Chimie**, 6 (2003) 1153-1164.
- [14] Ganesan V, Walcarius A, *Surfactant Templated Sulfonic Acid Functionalized Silica Microspheres as New Efficient Ion Exchangers and Electrode Modifiers*, **Langmuir**, 20 (2004) 3632-3640.
- [15] Klemperer G W, Mainz V V, Ramamurthi S D, Rosenberg S F, In: Brinker E D, Clark E D, Ulrich R D. *Better ceramics through chemistry III*, vol. 121. Pittsburgh P A' Materials Research Society; 1988. p. 15.
- [16] Cuiming W, Tongwen Xu, Weihua Y, *Fundamental studies of a new hybrid (inorganic–organic) positively charged membrane: membrane preparation and characterizations*, **J Membr Sci**, 216 (2003) 269-278.
- [17] Cuiming W, Tongwen Xu, Weihua Y, *A new inorganic-organic negatively charged membrane: membrane preparation and characterizations*, **J Membr Sci**, 224 (2003) 117-125.
- [18] Kogure M, Ohya H, Patrson R, *Properties of new inorganic membranes prepared by metal alkoxide methods Part II: New inorganic-organic anion-exchange membranes prepared by the modified metal alkoxide methods with silane coupling agents*, **J Membr Sci**, 126 (1997) 161-169.
- [19] Vyas P V, Shah B G, Trivedi G S, Ray P, Adhikary S K, Rangarajan R, *Characterization of heterogeneous anion-exchange membrane*, **J Membr Sci**, 187 (2001) 39-46.
- [20] Winston H W S, Sarkar K K, (editors) *Membrane handbook*. New York' Van Nostrand Reinhold; (1992).
- [21] Mark H F, Gaylord N G, *Encyclopedia of Polymer Science and Technology*, vol 8, New York, Wiley; (1968), 633.
- [22] Nezhadali A, *Selective transport of copper(II) ion across a polymer membrane incorporating a difunctional schiff-base ionophore*, **J Inclusion Phenomena Macrocyclic Chem**, 54 (2006) 307–308.

- [23] Gode F, Pehlivan E, *A comparative study of two chelating ion-exchange resins for the removal of chromium(III) from aqueous solution*, **J Hazard Mater**, 100 (2003) 231-243.
- [24] Demirbas A, Pehlivan E, Gode F, Altun T, Arslan G, *Adsorption of Cu(II), Zn(II), Ni(II), Pb(II) and Cd(II) from aqueous solution on Amberlite IR-120 synthetic resin*, **J Collo Inter Sci**, 282 (2005) 20-25.
- [25] Xu D, Katsu T, *Lead-selective membrane electrode based on dibenzyl phosphate*, **Anal Chim Acta**, 401 (1999) 111-115.
- [26] Yang X, Kumar N, Hibbert D B, Alexander P W, *Lead(II)-selective membrane electrodes based on 4,7,13,16-Tetrathienoyl-1,10-dioxo-4,7,13,16-tetraazacyclooctadecane*, **Electroanalysis**, 10 (1998) 827-831.
- [27] Bromberg L, Levin G, Kedem O, *Transport of metals through gelled supported liquid membranes containing carrier*, **J Membr Sci**, 71 (1992) 41–50.
- [28] de Gyves J, de San Miguel E R, *Metal ion separations by supported liquid membranes*, **Ind Eng Chem Res**, 38 (1999) 2182–2202.
- [29] Nazarenko A Y, Lamb J D, *Selective transport of lead(II) and strontium(II) through a crown ether-based polymer inclusion membrane containing dialkyl-naphthalenesulfonic acid*, **J Inclusion Phenom**, 29 (1997) 247–258.
- [30] Walkowiak W, Bartsch R A, Kozłowski C, Gega J, Charewicz W A, Amiri-Eliasi B, *Separation and removal of metal ionic species by polymer inclusion membranes*, **J Radioanal Nucl Chem**, 246 (2000) 643–650.
- [31] Lamb J D, Nazarenko A Y, *Lead(II) ion sorption and transport using polymer inclusion membranes containing tri-octylphosphine oxide*, **J Membr Sci**, 134 (1997) 255–259.
- [32] Brzozka Z, Pietraszkiewicz M, *Mercury ion-selective polymeric membrane electrodes based on substituted diaza crown ethers*, **Electroanalysis**, 3 (1991) 855-858.
- [33] Aguilar J C, Sanchez-Castellanos M, de San Miguel E R, de Gyves J, *Cd(II) and Pb(II) extraction and transport modeling in SLM and PIM systems using Kelex 100 as carrier*, **J Membr Sci**, 190 (2001) 107–118.
- [34] Krakowiak K E, Bradshaw J S, Zamecka-Krakowiak D J, *Synthesis of aza-crown ethers*, **Chem Rev**, 89 (1989) 929–972.

- [35] Guo X, Zhai F, Fang J, Laguna M F, Lopez-Gonzalez M, Riande E, *Permselectivity and conductivity of membranes based on sulfonated naphthalenic copolyimides*, **J Phys Chem B**, 111 (2007) 13694–13702.
- [36] Sata T, Sata T, Yang W, *Studies on cation-exchange membranes having permselectivity between cations in electro dialysis*, **J Memb Sci**, 206 (2002) 31-60.
- [37] Sata T, Ishii Y, Kawamura K, Matsusaki K, *Composite membranes prepared from cation exchange membranes and polyaniline and their transport properties in electro dialysis*, **J Electrochem Soc**, 146 (1999) 585-591.
- [38] Vyas P V, Ray P, Rangarajan R, Adhikary S K, *Electrical conductance of heterogeneous cation-exchange membranes in electrolyte solutions*, **J Phys Chem B**, 106 (2002) 11910–11915.
- [39] Gohil G S, Nagarale R K, Binsu V V, Shahi V K, *Preparation and characterization of monovalent cation selective sulfonated poly(ether ether ketone) and poly(ether sulfone) composite membranes*, **J Collo Inter Sci**, 298 (2006) 845-853.
- [40] Saxena A, Gohil G S, Shahi V K, *Electrochemical membrane reactor: single step separation and ion substitution for the recovery of lactic acid from lactate salts*, **Ind Eng Chem Res**, 46 (2007) 1270-1276.
- [41] Hickner M A, Ghassami H, Kim Y S, Einsla B R, McGrath J E, *Alternative polymer systems for proton exchange membranes (PEMs)*, **Chem Rev**, 104 (2004) 4587-4612.
- [42] Kumar M, Tripathi B P, Shahi V K, *Ionic transport phenomenon across sol–gel derived organic–inorganic composite mono-valent cation selective membranes*, **J Memb Sci**, 340 (2009) 52–61.
- [43] Schuster M, Meyer W H, Wenger G, Herz H G, Ise M, Achuster M, Kreuer K D, Maier J, *Proton mobility in oligomer-bound proton solvents: imidazole immobilization via flexible spacers*, **Solid State Ionics**, 145 (2001) 85-92.
- [44] Jacob S, Cohet S, Poinson C, Popall M, *Proton conducting inorganic–organic matrices based on sulfonyl- and styrene derivatives functionalized polycondensates via sol–gel processing*, **Electrochim Acta**, 48 (2003) 2181-2186.

- [45] Depre L, Ingram M, Poinsignon C, Popall M, *Proton conducting sulfon/sulfonamide functionalized materials based on inorganic–organic matrices*, **Electrochim Acta**, 45 (2000) 1377-1383.
- [46] Williams C J, Aderhold D, Edyvean G J, *Comparison between biosorbents for the removal of metal ions from aqueous solutions*, **Water Res**, 32(1998)216–224.
- [47] Juttner K, Galla U, Schmieder H, *Electrochemical approaches to environmental problems in the process industry*, **Electrochim Acta**, 45(2000)2575–2594.
- [48] Kadirvelu K, Thamaraiselvi K, Namasivayam C, *Removal of heavy metals from industrial wastewaters by adsorption onto activated carbon prepared from an agricultural solid waste*, **Bioresour Technol**, 76(2001)63–65.
- [49] Janssen L J J, Koene L, *The role of electrochemistry and electrochemical technology in environmental protection*, **Chem Eng J**, 85(2002)137–146.
- [50] Adhoum N, Monser L, Bellakhal N, Belgaied J E, *Treatment of electroplating wastewater containing Cu(II), Zn(II) and Cr(VI) by electrocoagulation*, **J Hazard Mater**, 112(2004)207–213.
- [51] Laatikainen M, Sirola K, Paatero E, *Binding of transition metals by soluble and silica-bound branched poly(ethyleneimine). II Binding kinetics in silicabound BPEI*, **Colloids Surf A**, 296(2007)158–166.
- [52] Sirola K, Laatikainen M, Lahtinen M, Paatero E, *Removal of copper and nickel from concentrated ZnSO₄ solutions with silica-supported chelating adsorbents*, **Sep Purif Technol**, 64 (2008) 88–100.
- [53] Helfferich, *Ion-Exchange*, Dover Publications, New York, 1962, Chapter 6.
- [54] Liu C.X, Bai R.B, *Adsorptive removal of copper ions with highly porous chitosan/cellulose acetate blend hollow fiber membranes*, **J Membr Sci**, 284(2006)313–322.
- [55] Cheng Z, Liu X, Han M, Ma W, *Adsorption kinetic character of copper ions into a modified chitosan transparent thin membrane from aqueous solution*, **J Hazard Mater**, 182 (2010) 408–415.
- [56] Gibbs G, Tobin J M, Guibal E, *Influence of chitosan pre protonation on reactive block 5 sorption isotherms and kinetics*, **Ind Eng Chem Res**, 43 (2004)1–11.

- [57] Jin L, Bai R B, *Mechanisms of lead adsorption on chitosan/PVA hydrogen beads*, **Langmuir**, 18 (2002) 9765–9770.
- [58] Akita S, Sastillo L P, Nii S, Takahashi K, Takeuchi H, *Separation of Co(II)/Ni(II) via micellar-enhanced ultrafiltration using organophosphorus acid extractant solubilized by nonionic surfactant*, **J Membr Sci**, 162(1999)111–117.
- [59] Ismael M, Tondre C, *Kinetically controlled separation of nickel(II) and cobalt(II) using micelle-solubilized extractant in membrane processes*, **Langmuir**, 8(1992)1039–1041.
- [60] Nagarale R K, Gohil G S, Shahi V K, Rangarajan R, *Preparation of organic–inorganic composite anion-exchange membranes via aqueous dispersion polymerization and their characterization*, **J Collo Interf Sci**, 287(2005)198–206.
- [61] Shahi V K, Muruges A P, Makwana B S, Thampy S K, Rangarajan R, *Comparative investigations on electrical conductance of ion-exchange membranes*, **Ind J Chem**, 39A (2000) 1264-1269.
- [62] Nagarale R K, Shahi V K, Thampy S K, Rangarajan R. *Studies on electrochemical characterization of polycarbonate and polysulfone based heterogeneous cation-exchange membranes*, **React Funct Polym**, 61 (2004) 131-138.
- [63] Koter S, Piotrowski P, Kerres J. *Comparative investigations of ion-exchange membranes*, **J Membr Sci**, 153 (1999) 83-90.
- [64] Lehmani A, Turq P, Perie M, Perie J, Simonin J P, *Ion transport in Nafion[®] 117 membrane*, **J Electroanal Chem**, 428 (1997) 81-89.
- [65] Shahi V K, Trivedi G S, Thampy S K, Rangarajan R, *Studies on the electrochemical and permeation characteristics of asymmetric charged porous membranes*, **J Colloid Interface Sci**, 262 (2003) 566-573.
- [66] Li Q, Jensen J O, Savinell R F, Bjerrum N J, *High temperature proton exchange membranes based on polybenzimidazoles for fuel cells*, **Progr Polym Sci**, 34 (2009) 449-477.
- [67] Tripathi B P, Shahi V K, *3-[[3- Triethoxysilyl)propyl]amino]propane-1-sulfonic acid-poly(vinyl alcohol) cross-linked zwitterionic polymer electrolyte*

- membranes for direct methanol fuel cell applications, **Applied Mat Interface**, 1 (2009) 1002-1012.
- [68] Chen V, Lib H, Fane A G, *Non-invasive observation of synthetic membrane processes – a review of methods*, **J Membr Sci**, 241 (2004) 23-44.
- [69] Silva R F, Francesco M D, Pozio A, *Tangential and normal conductivities of Nafion[®] membranes used in polymer electrolyte fuel cells*, **J Power Sources**, 134 (2004) 18-26.
- [70] Alcaraz1 A, Holdika H, Ruffing T, Ramo A, Rez P, Mafe S, *AC impedance spectra of bipolar membranes: an experimental study*, **J Membr Sci**, 150 (1998) 43-56.
- [71] Coster H G L, Chilcott T C, Coster A C F, *Impedance spectroscopy of interfaces, membranes and ultrastructures*, **Bioelectrochemistry and Bioenergetics**, 40 (1996) 79-98.
- [72] Coster H G L, Kim K J, Dahlan K, Smith J R, Fell C J D, *Characterisation of ultrafiltration membranes by impedance spectroscopy. I. Determination of the separate electrical parameters and porosity of the skin and sublayers*, **J Membr Sci**, 66 (1992) 19-.
- [73] Singh K, Shahi V K, *Impedance spectral studies of cholesterol lecithin mixture*, **Indian Journal of Chemistry**, **Ind J Chem**, 34A (1994) 268-272.
- [74] Tian Z W, *Study methods of electrochemistry*. China' Scientific Publications; 1985. p. 274.
- [75] Watkins E J, Pfromn P H, *Capacitance spectroscopy to characterize organic fouling of electrodialysis membranes*, **J Membr Sci**, 162 (1999) 213-218.
- [76] Vazquez M I, Banavente J, *A study of temperature effect on chemical, structural and transport parameters determined for two different regenerated cellulose membranes*, **J Membr Sci**, 219 (2003) 59-67.
- [77] Oleinikova M, Mun˜oz M, Benavente J, Valiente M, *Evaluation of Structural Properties of Novel Activated Composite Membranes Containing Organophosphorus Extractants as Carriers*, **Langmuir**, 16 (2000) 716-721.
- [78] Chilcott T C, Chan M, Gaedt L, Nantawisarakul T, Fane A G, Coster H G L, *Electrical impedance spectroscopy characterisation of conducting membranes: I. Theory*, **J Membr Sci**, 195 (2002) 153-167.

- [79] Gaedt L, Chilcott T C, Chan M, Nantawisarakul T, Fane A G, Coster H G L, *Electrical impedance spectroscopy characterisation of conducting membranes: II. Experimental*, **J Membr Sci**, 195 (2002) 169-180.
- [80] Sata T, *Studies on anion exchange membranes having permselectivity for specific anions in electrodialysis - effect of hydrophilicity of anion exchange membranes on permselectivity of anions*, **J Membr Sci**, 167 (2000) 1-31.
- [81] Singh S, Jasti A, Kumar M, Shahi V K, *A green method for the preparation of highly stable organic-inorganic hybrid anion-exchange membranes in aqueous media for electrochemical processes*, **Polym Chem**, 1 (2010) 1302-1312.
- [82] Shahi V K, Thampy S K, Rangarajan R, *Studies on transport properties of surfactant immobilized anion-exchange membrane*, **J Membr Sci**, 158 (1999) 77-83.
- [83] Singh K, Shahi V K, *Studies on electrochemical characterization of ion selective cellulose acetate membranes with and without a lecithin liquid membrane*, **J Membr Sci**, 49 (1990) 223-233.
- [84] Singh K, Shahi V K. *Electrochemical studies on Nation membrane*, **J Membr Sci**, 140 (1998) 51-56.
- [85] Lashminarayanaiah N. *Transport phenomena in membranes*. New York' Academic Press; 1969. p. 64.
- [86] Shahi V K, Makawana B S, Thampy S K, Rangarajan R, *Electrochemical characterization of cation exchange membrane with immobilized anionic and cationic surfactants*, **Ind J Chem**, 38A (1999) 124-128.
- [87] Singh K, Tiwari A K, *Studies on ion exchange membranes with permselectivity for specific ions in electrodialysis*, **J Membr Sci**, 34 (1987) 155-163.
- [88] Kumar M, Singh S, Shahi V K, *Cross-linked poly(vinyl alcohol)-poly(acrylonitrile-co-2-dimethylamino ethylmethacrylate) based anion-exchange membranes in aqueous media*, **J Phys Chem B**, 114 (2010) 198-206.
- [89] Ngah, W S W, Ghani, S A, Kamari A, *Adsorption behaviour of Fe(II) and Fe(III) ions in aqueous solution on chitosan and cross-linked chitosan beads*. **Bioreso Technol**, 96 (18)(2005) 443-448.

- [90] Ng, J.C.Y.; Cheung, W.H. G., *Equilibrium studies for the sorption of lead from effluents using chitosan*. **Chemosphere**, 52(6)(2003)1021-1029.
- [91] Vogel A I, *Quantitative Inorganic Analysis*, 3rd ed., Longmans, London, (1961) 324.
- [92] Acar M H, Bicak N, *Synthesis of hexylated triethylenetetramine: new ligand for homogeneous atom transfer radical polymerization*, **J Polym Sci, Part A: Polym Chem**, 41 (2003) 1677–1680.
- [93] Hill M L, Kim Y S, Einsla B R, McGrath J E, *Zirconium hydrogen phosphate/disulfonated poly(arylene ether sulfone) copolymer composite membranes for proton exchange membrane fuel cells*, **J Membr Sci**, 283(2006)102–108.
- [94] Tan N, Xiao G, Yan D, Sun G, *Preparation and properties of polybenzimidazoles with sulfophenylsulfonyl pendant groups for proton exchange membranes*, **J Membr Sci**, 353(2010) 51–59.
- [95] Fu R Q, Woo J J, Seo S J, Lee J S, Moon S H, *Covalent organic/inorganic hybrid proton-conductive membrane with semi-interpenetrating polymer network: preparation and characterizations*, **J Power Sources**, 179(2008)458–466.
- [96] Tripathi B.P., Kumar M., Shahi V.K., *Highly stable proton conducting nanocomposite polymer electrolyte membrane (PEM) prepared by pore modifications: an extremely low methanol permeable PEM*, **J Membr Sci**, 327 (2009)145–147.
- [97] Wu Y., Wu C., Xu T., Yu F., Fu Y., *Novel anion-exchange organic–inorganic hybrid membranes: preparation and characterizations for potential use in fuel cells*, **J Membr Sci**, 321 (2008) 299–308.
- [98] Xiong Y, Liu Q L, Zeng Q H, *Quaternized cardopolyether ketone anion exchange membrane for direct methanol alkaline fuel cells*, **J Power Sources**, 193(2009)541–546.
- [99] Singh S, Patel P, Shahi V K, Chudasama U, *Pb²⁺ selective and highly crosslinked zirconium phosphonate membrane by sol–gel in aqueous media for electrochemical applications*, **Desalination**, 276 (2011) 175–183.
- [100] Marion M C, Garbowski E, Primet M, *Physicochemical properties of copper oxide loaded alumina in methane combustion*, **J Chem Soc, Faraday Trans**, 86 (1990) 3027-3030.

- [101] Erdem E, Karapinar N, Donat R, *The removal of heavy metal cations by natural zeolites*, **J Collo Inter Sci**, 280 (2004) 309–314.
- [102] Katchalsky A, Curran P F, (1965), *Nonequilibrium thermodynamics in biophysics*, Harvard Univ. Press, Cambridge.
- [103] Baes C F, Mesmer R E, (1976), *The Hydrolysis of Cations*, Wiley, New York.
- [104] Onsoyen, E, Skaugrud O, *Metal recovery using chitosan*, **J Chem Technol Biotechnol**, 49(1990)395-401.
- [105] Bajpai D N, *Advanced Physical Chemistry*, S. Chand and Company, New Delhi, India, (1998).
- [106] Saeed A, Iqbal M, Waheed M W, *Removal and recovery of lead(II) from single and multimetal (Cd, Cu, Ni, Zn) solutions by crop milling waste (black gram husk)*, **J Hazard Mater**, 117 (1) (2005) 65-69.
- [107] Itoyama B K, Tokura S, Hayashi T, *Lipoprotein-lipase immobilization onto porous chitosan beads*, **Biotechnol Prog**, 10 (1994) 225-229.
- [108] Sankararamkrishnan N, Sharma, A K, Sanghi R, *Novel chitosan derivative for the removal of cadmium in the presence of cyanide from electroplating wastewater*, **J Hazard Mater**, 148(1-2)(2007)353-359.
- [109] Dantas T N C, Neto A A D, Moura M C P A, Neto E L B, Telemaco E P, *Chromium adsorption by chitosan impregnated with microemulsion*, **Langmuir**, 17(1)(2001)4256-4261.
- [110] Chatterjee S, Chatterjee B P, Guha A K, *Adsorptive removal of Congo red, a carcinogenic textile dye by chitosan hydrobeads: binding mechanism, equilibrium and kinetics*, **Collo Surfa A: Physicochem. Eng. Aspects**, 299(1-3)(2007)146-153.
- [111] Namasivayam C, Ranganathan K, *Removal of Cd (II) from wastewater by adsorption on “waste” Fe(III)/Cr(III) hydroxide*. **Water Res**, 29(7) (1995)1737-1745.
- [112] Kannamba B, Reddy K L, AppaRao B V, *Removal of Cu(II) from aqueous solutions using chemically modified chitosan*. **J Hazard Mater**, 175(1-3) (2010)939-945.
- [113] Felse P A, Panda T, *Studies on applications of chitin and its derivatives*. **Bioprocess Eng**, 20(1999)505-510.